



BRNO UNIVERSITY OF TECHNOLOGY

VYSOKÉ UČENÍ TECHNICKÉ V BRNĚ

FACULTY OF CIVIL ENGINEERING

FAKULTA STAVEBNÍ

INSTITUTE OF GEODESY

ÚSTAV GEODÉZIE

**GEOPHYSICAL METHODS OF INTEGRATION OF THE
LOCAL VERTICAL DATUMS INTO WORLD HEIGHT
SYSTEM**

GEOFYZIKÁLNE METÓDY ZAČLENENIA LOKÁLNYCH VÝŠKOVÝCH SYSTÉMOV
DO CELOSVETOVÉHO VÝŠKOVÉHO SYSTÉMU

DOCTORAL THESIS

DIZERTAČNÁ PRÁCA

AUTHOR

AUTOR PRÁCE

Ing. Michal Buday

SUPERVISOR

VEDÚCI PRÁCE

prof. Ing. VILIAM VATRT, DrSc.

BRNO 2020

CONTENTS

Introduction	3
Goals of the doctoral thesis	4
1 Theoretical Background	5
1.1 Overview of the current state of selected height systems used over the world	5
1.2 Theoretical background for strategy of setting out the vertical reference frame	5
1.3 Basic principle of acquiring the reference surface - GBVP	7
1.4 Geoid	7
1.4.1 Frequency components of the geoid	8
1.4.2 Orthometric heights	9
1.5 Detailed look at the Molodensky's problem	9
1.5.1 Quasi-geoid	9
1.5.2 Molodensky's problem - free boundary value problem	10
1.5.3 Molodensky's problem - fixed boundary value problem	11
1.6 Computing the connection between Local Vertical Datum and Global Vertical Reference Frame	12
1.7 'FAST' GBVP connection to WHS	13
1.7.1 The definition of the level ellipsoid	14
1.7.2 The permanent tide role in height systems and transformation between them	15
1.8 Residual terrain modelling	16
1.9 Gravity field modelling	16
1.9.1 Terrain effects	17
1.10 Mean elevation surface	17
1.10.1 Harmonic correction	18
1.11 Remove-Compute-Restore Technique	19
2 The case study for the territories of the Czech Republic and the Slovak Republic	20
2.1 Input data	20
2.2 Adjustment process	20
2.3 Results by FAST GBVP	21
2.3.1 Models - FAST GBVP	23
2.4 Classical GBVP approach	26
2.5 RTM contribution	26
2.5.1 Models - classic GBVP	27
3 Conclusions and outlook	34
3.1 Summary of results	34
3.2 Recommendations for future work	35
3.3 Contribution of the doctoral thesis	36
3.4 PHYSGEO package	36
Bibliography	37
Publications of the author	41
Curriculum Vitae	43

INTRODUCTION

Almost every country in the World set up its own Vertical Datum (VD). These datums differ from each other in the origin of each Vertical Datum, the theory used of the basic surface which the heights are measured from or in the way how they deal with Earth's tides. One of the major breakthroughs to set up the unified Global Vertical Reference Frame (GVRF) was the determination of the constant W_0 ([1], [2],[3], [4]). The constant represents the value of the gravity potential on the geoid surface, the geopotential equipotential surface of the Earth's gravity field which best fits, in a least-squares adjustment sense, the global mean sea level. Excluding the GNSS measurements, all the other determinations of the physical heights are strongly dependent on the Earth's gravity field, its shape and magnitude.

The Earth's gravity field can be split into two independent components, the first one is the gravitational component and the second one is the centrifugal part. For calculating the centrifugal part of the gravity it is necessary to know the position of an arbitrary point with relevance to the axis of the rotation and angular speed of the rotary motion. The gravitational component is the one that is challenging to determine. If Newton's law of gravitation is taken into consideration, this direct computation of the attraction force is not possible. The reason for this is that there are no sufficient data. For precise modelling, the detailed shape of the Earth must be known, also the density distribution inside the Earth plays a crucial role. The global gravitational field models are based namely on terrestrial and satellite gravimetry, satellite gradiometry and satellite altimetry.

The satellite missions such as GOCE([5]), GRACE([6]) and CHAMP ([7]) are well known for their abilities to measure the components of the gravity field - the first and second derivatives of the gravitational potential. Biggest advantage of the satellite measurements is the global coverage (except the area of South and North pole). Their disadvantage is their spatial resolution, the most modern models are computed up to degree and order 300 ([8],[9]). The approximate spatial resolution of such model is 67 km, which means that the higher frequencies are missing. For determining the short-wave characteristics of the gravity field, the terrestrial gravity data and the gravity data from the aerial survey are commonly used. Combining all available data, the global gravity field models (GGFMs) are produced nowadays such as EIGEN-6C4([10]), GECO([11]), EGM08([12]). The latest models are using Stokes' coefficients up to degree and order 5540, such as XGM2019e ([13]).

The gravitational field is a conservative potential field and quantity used to describe is called gravitational potential. Based on the potential theory, the gravitational potential outside the masses of the Earth can be expressed as an infinite series of spherical harmonics and such series is represented by a set of spherical coefficients. Using a set of coefficients with four fundamental constants in geodesy GM (geocentric gravitational constant), ω (speed of the Earth's rotary motion), J_2 (second Stokes' zonal coefficient) and W_0 can lead to the definition of the Global Vertical Reference Frame. Because any model can be only an approximation of the reality, the theoretical infinite harmonic series is cut off at some degree n and the remaining coefficients are neglected.

For the purpose of this doctoral thesis, the GVRF is represented by GGFM and previously mentioned four fundamental constants in geodesy. Because the directly measured terrestrial gravity data are very problematic to obtain for the territories of the Czech Republic and the Slovak Republic, the alternate approach is suggested. To obtain the highest possible frequencies of the gravity signals, the method of residual terrain modelling was chosen. It means that the GGFM's Stokes' coefficients are used up to maximum possible degree and order and the higher frequencies are computed using forward gravity field modelling and suitable terrain model. For example, for the model EGM08 the dataset of surface $5' \times 5'$ gravity anomalies is related to the global elevation model DTM2006.0. This elevation model serves as a common surface for all gravity anomalies and is also used consistently in the computation of all terrain-related quantities necessary for the pre-processing of the gravity data and for the subsequent use of EGM08. This can be translated as follows: To perform a spectral combination, for example, the combination of gravity disturbances computed from EGM08 and higher frequencies of the gravity signal, modelled from the digital elevation model, only those topography masses between the mean elevation surface represented by DTM2006.0 and the topography should be taken into account. This process was done using the DEM model of GMTED10 ([14]) in its finest resolution. For the cases where the real topography is below the mean elevation surface, the question what to do about the harmonic correction rises. In these cases, the harmonic correction plays a role, and the available model is capable to model gravity outside the masses as a harmonic function and inside the masses as a non-harmonic function. The geopotential models expressed in the form of spherical harmonics are not capable of handling the non-harmonic part. Thus, the non-harmonicity

of functions inside the masses should not be corrected.

Goals of the doctoral thesis

Since independent countries are using their own independent vertical reference frames, the main aim of this doctoral thesis is to provide the outline for the unification of local vertical datums, especially using the methods based on solving the geodetic boundary value problems, global gravity field models and GNSS/levelling sites. To accomplish the main goal, the following steps will be discussed:

- Short summary of historical development of the Local vertical datums for the territories of the Czech Republic and the Slovak Republic.
- A description of the current state of development.
- Characteristic of different types of physical heights which are used worldwide.
- Characteristic of available data for creation of GVRF, such as global gravity field models, discrete gravity data, digital elevation models, GNSS/levelling sites, etc.
- The role of the permanent tide systems in the realisation of the vertical reference frame. Also, provide a brief overview of the transformation between various types of tidal systems will be provided.
- Derivation of the mathematical framework for creating the GVRF.
- Definition of the geodetic boundary value problem with Dirichlet's and Newton's boundary problem.
- Provide the mathematical framework for dealing with topographic masses and also describe the mathematical framework for Residual Terrain Modelling.
- Summary of distribution GNSS/levelling benchmarks, available gravity data for the territories of the Czech Republic and the Slovak Republic.
- Provide a case study of realization of the GVRF for the territories of the Czech Republic and the Slovak Republic while using the fundamental constants in Geodesy.

To be able to practically achieve the above-outlined goals it is necessary to have appropriate software available. **The source codes** dedicated to numerical computations created for the purpose of this doctoral thesis **will be provided publicly and free of charge under the MIT licence.**

1 THEORETICAL BACKGROUND

1.1 Overview of the current state of selected height systems used over the world

The creation of a unified height system is a long-lasting discussion in geodesy. There are suitable global applications which are focused on the realization of the Unified Vertical Reference System - World Height System (WHS) (see [15], [16], [17]) and also many regional applications, that differ for individual regions (for example Europe [18], Australia [19], New Zealand [20], etc).

The importance of this task is supported by the joint effort of scientists all around the globe. The intermediate step to achieve the goal to unify the vertical datums is to create one common joint reference frame for the individual continents.

The joint project for Africa continent is the African Geoid Project (AGP) and is an attempt to produce a uniform precise geoid model for Africa. The result of this project is geoid model AGP2007 (published [21]) which together with GNSS measurements are part of African Geodetic Reference Frame (AFREF).

For the continent of South America the initiative called Sistema de Referencia Geocéntrico para las Américas (SIRGAS) was established during the IAG Scientific Assembly in 1997 ([22]). Its main objective is to define a modern unified vertical reference system for SIRGAS. Therefore, the goal is to establish the corresponding reference frame and to transform the existing LVDs to this new set up vertical datum.

Similarly the North American Vertical Datum of 1988 (NAVD88) ([23]) was established in 1991 for the continent of North America. The NAVD 88 was established by the minimum-constrained adjustment of the Canadian-Mexican-United States levelling observations. It held fixed the height of the primary tidal bench mark, referenced to the new International Great Lakes Datum of 1985 local mean sea level height value, at Father Point/Rimouski, Quebec, Canada.

The brief overview of current state of height systems used in Europe is shown in table 1.1. It is clearly visible that there are unique LVDs across Europe which are using different height types, reference tide gauges or adopted tidal systems.

1.2 Theoretical background for strategy of setting out the vertical reference frame

The creation of the global unified vertical reference frame is one of the main tasks of the International Association of Geodesy (IAG). The Global Geodetic Observing System (GGOS) of the IAG takes care and provides a precise geodetic infrastructure for monitoring of the dynamic System Earth by quantifying our planet's changes in space and time. Which promotes the standardization of height systems worldwide. The special part of GGOS which is focusing on this task is GGOS Focus Area Unified Height System (GGOS-FA-UHS). The main result is the compilation of the IAG resolution for the 'Definition and realization of an International Height Reference System (IHRS)' approved during the 2015 General Assembly of the International Union of Geodesy and Geophysics (IUGG) in Prague, Czech Republic. Currently the chairman of this committee is Laura Sánchez ¹. The technical reports suggesting the realisation of the vertical reference frame are [25], [26].

Rummel in his study [27] stated that there are three possible ways how to achieve the goal of vertical datum unification. The first strategy proposed by him is the *direct connection by levelling and gravimetry*. This method, however, can only be applied for those local datums which are connected via land - e.g., for example, the common adjustment of the 27 national European levelling networks so-called *UELN* (United European Levelling Network²). The second strategy overcomes the disadvantage of a direct connection by land and it is called *the oceanographic approach*. This approach is done by oceanic levelling ([28]). The basic principle is based on usage of the satellite altimetry to determine the height of the mean sea level (above or below geoid). By combining the measured data with global gravity field models and other oceanographic models (such as density model, temperature model, etc.), the relative datum offset is obtained. The third proposed strategy is solving the *geodetic boundary*

¹Deutsches Geodätisches Forschungsinstitut, Technische Universität München, Germany

²This common adjustment was done in the units of gravity potential m^2s^{-2} to avoid dealing with different height systems across the Europe

Tab. 1.1: Height reference frame unification in Europe: Estimated offsets from gravity field (GF) approach based on the filter-combined GOCO03S+EGG2008 gravity field model and geodetic levelling approach. All values refer to U_0 of GRS80 and are computed in zero-tide system [24] - modified table and description by [author].

Country	Adopted tidal system	GF	Geodetic Levelling	Reference tide gauge	Heights type
		[m]	[m]		
Austria	mean	-0.269	-0.350	Trieste	norm.-orthometric
Bulgaria	mean	+0.304	+0.213	Kronstadt	normal
Croatia	mean	-0.259	-0.328	Trieste	norm.-orthometric
Czechia	mean	+0.149	+0.115	Kronstadt	normal
Denmark	tide-free	-0.069	-0.019	10 different TG	orthometric
Finland	zero	-0.033	-0.024	Amsterdam	normal
France	mean	-0.494	-0.486	Marseilles	normal
Germany	mean	+0.000	+0.000	Amsterdam	normal
Great Britain	mean	-0.418	+0.030	Newlyn	norm.-orthometric
Hungary	mean	+0.214	+0.147	Kronstadt	normal
Italy	mean	-0.155	-0.291	Genoa	orthometric
Latvia	mean	0.129	0.139	Kronstadt	normal
Lithuania	mean	0.119	0.106	Kronstadt	normal
Netherlands	tide-free	-0.029	0.009	Amsterdam	no-gravity correction
Norway	zero	-0.056	-0.023	Amsterdam	normal
Poland	tide-free	0.211	0.156	Kronstadt	normal
Portugal	mean	-0.311	-0.265	Cascais	orthometric
Romania	mean	0.125	0.047	Constanta	normal
Slovakia	mean	0.198	0.126	Kronstadt	normal
Slovenia	mean	-0.331	-0.402	Trieste	norm.-orthometric
Spain	mean	-0.433	-0.501	Alicante	norm.-orthometric
Sweden	zero	-0.042	-0.023	Amsterdam	normal
Switzerland	mean	-0.108	-0.143	Pierres du Niton	norm.-orthometric

value problem (GBVP). This method connects the local disjointed vertical datums and also provides the Local Vertical Datums (LVDs) offsets. The GBVP approach with multiple vertical datums was developed and investigated by [29], [30], [31], [32], [33].

One of the most important values for determining the global vertical reference frame is W_0 , the value of the gravity potential on the geoid's surface. This value was computed using fixed GBVP in ocean areas. **The first value of W_0 that IUGG agreed on is $62\,636\,856.0\text{ m}^2\text{s}^{-2}$** [34], [35]. The latest value is set to $W_0 = 62\,636\,853.4\text{ m}^2\text{s}^{-2}$ [4], but this value **is not accepted** by IUGG.

The LVDs are based on the computation of local geoid or quasi-geoid models and these models are based on Stokes' integration with corresponding gravity data. To create global vertical datum, the connection between local data and the Global Gravity Field Models (GGFMs) is required.

A different approach is to combine the GGFM of the highest spherical harmonics degree with the local gravity anomalies and digital elevation models (such as SRTM data [36]) with high resolution for computation of the topographic contribution to gravity measurements and gravity data.

As it was mentioned above, all the national height reference systems are based on levelling networks combined with gravimetry. For each height reference system, the fixed datum point is required with the basic reference level from which the heights are measured as a length of the vertical or plumbline between the reference surface (geoid, quasi-geoid³) and point on the Earth's surface. The fixed datum points - the tide gauges stations - are usually used. On these stations, the sea level is observed over a long period of time and the value of mean sea level is obtained. This value is strongly dependent on the geopotential value on the level surface which the tide gauge is placed on.

The gravity field approach uses the information of GNSS/levelling benchmarks such as ellipsoidal heights, their global position and the physical heights in the LVD. Height datum offsets are then calculated by comparing the biased undulations resulting from GNSS/levelling data with corresponding unbiased undulations derived from independent gravity field information.

³Quasi-geoid is not an equipotential surface and does not have a special meaning in geophysics.

1.3 Basic principle of acquiring the reference surface - GBVP

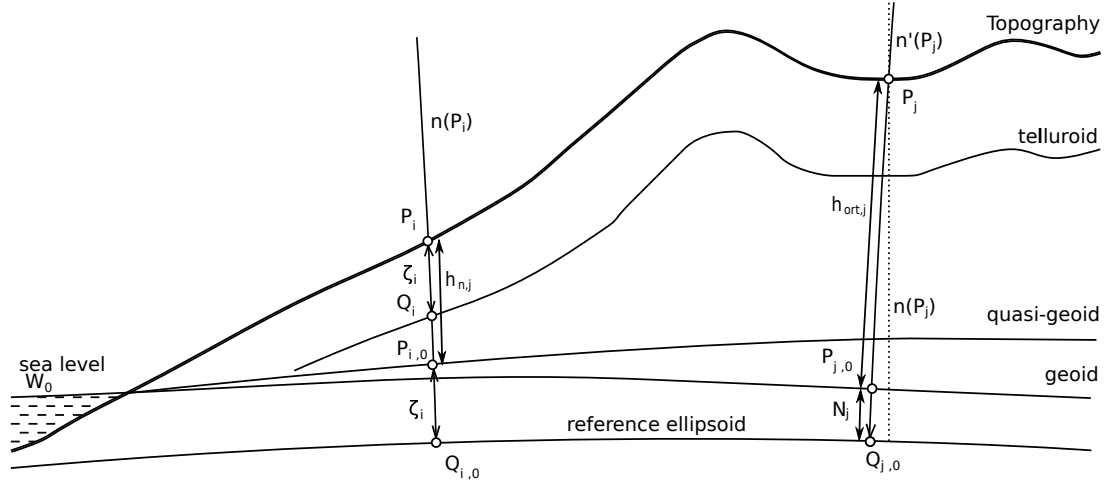


Fig. 1.1: Overview of the basic principle of physical heights [author].

The Figure 1.1 shows the two most common physical height types. The Molodensky's concept of normal heights and the Stokes' concept of the orthometric heights. The geoid ([37]) is an important equipotential surface used in geodesy and geophysics. The geoid serves as the ideal reference surface for height systems in all the countries that adopted the concept of the orthometric heights. The geometric interpretation is that h_{ort} is length of the plumbline between the geoid (point $P_{j,0}$) and point on the Earth's surface (point P_j). The geoidal normal n' is displayed with dotted line for point P_j . The angle between the normals n and n' is called deflection of the vertical at point P_j . Nowadays, the most used simplification of Stokes' solution is Helmert's Earth body regularization [38].

1.4 Geoid

The geoid as a fundamental surface for the orthometric heights. The original idea is credited to C. F. Gauss. The name of the surface is credited J. B. Listing. The geoid is a continuous, smooth and convex closed surface, and also is the equipotential surface of the Earth's gravity field which best fits, in a least squares sense, global mean sea level⁴.

The basic formula is

$$h_{el} = N + h_{ort}, \quad (1.1)$$

where h_{el} stands for ellipsoidal height⁵, N is the geoid undulation and h_{ort} is orthometric height. To determine the basic level surface such as geoid, the geodetic boundary value problem has to be solved. This leads to the boundary value problem of Newton's type. The Newton's BVP ([39]) is defined as follows

$$\begin{aligned} \Delta T(\vec{r}) &= 0 & \text{for } \|\vec{r}\| > r_g \\ \left(\frac{\partial T}{\partial n_e} \right)_{P_0} - \frac{1}{\gamma_{Q_0}} \left(\frac{\partial \gamma}{\partial n_e} \right)_{Q_0} T(P_0) &= -\Delta g(P_0) & \text{on } \partial\Omega = S_g, \\ \lim_{\|\vec{r}\| \rightarrow \infty} T(\vec{r}) &= 0 \end{aligned} \quad (1.2)$$

⁴Even though we adopt a definition, that does not mean we are perfect in the realization of that definition. For example, in altimetry it is often used as a definition of the "mean sea level" in the oceans, but altimetry is not global method (missing the near polar regions). As such, the fit between "global" mean sea level and the geoid is not entirely conclusive. Also, there may be non-periodic changes in sea level (like persistent rise in sea level, for example).

⁵Length of the vertical between the reference ellipsoid and the point on the Earth's surface.

where S_g is the surface of the geoid as a boundary surface, T is the disturbing potential, n_e is normal/vertical line at point P and γ is normal gravity value, r_g is a radius of the sphere which approximates the geoid. The boundary condition is 2nd equation in 1.2, is also the fundamental equation in physical geodesy. In the case of the Stokes' GBVP, the Q_0 is point placed on the reference ellipsoid.

Considering the values on the boundary as known, we solve the disturbing T outside the boundary. The following equation 1.3 is the solution of the Newton's BVP on sphere⁶. We obtain the value of the disturbing potential

$$T(P_0) = \frac{\Delta GM}{r} + \frac{R}{4\pi} \iint_{\Omega} S(\psi_{P_0, \Omega}) \Delta g(\Omega) d\Omega, \quad (1.3)$$

where ΔGM is the unknown error of the adopted value of the geocentric mass constant, r is geocentric length for point P_0 , R is a radius of the geocentric sphere which roughly approximates geoid (often referred to as Brillouin sphere which is a sphere that includes all masses of the Earth), $S(\psi_{P_0, Q})$ is Stokes' kernel. The solution described in equation 1.3 is a spherical approximation where the integration domain Ω is the surface of the 'Brillouin sphere', the $d\Omega$ is an infinitesimal area of such sphere. In this case Ω is used as a dummy variable representing the position on the integration domain (in this case - reference sphere $\Omega = (\phi, \lambda)$, $-\pi/2 \leq \phi \leq \pi/2$, $0 \leq \lambda < 2\pi$)⁷. The equation describing the relation between the disturbing potential and gravity anomaly is often referenced as **fundamental geodetic equation**. The Stokes' function $S(\psi)$ (published in [37]) in its closed form is given by equation

$$S(\psi) = \frac{1}{\sin \frac{\psi}{2}} - 6 \sin \left(\frac{\psi}{2} \right) + 1 - 5 \cos \psi - 3 \cos \psi \cdot \ln \left(\sin \frac{\psi}{2} + \sin^2 \frac{\psi}{2} \right), \quad (1.4)$$

the Stokes' kernel can be also expressed in the form of an infinite series - spectral form ([41])

$$S(\psi) = \sum_{n=2}^{\infty} \frac{2n+1}{n-1} P_n(\cos \psi), \quad (1.5)$$

where ψ is obtained from spherical trigonometry ([42]) as the spherical distance (central angle) between the geocentric vectors of computation point and running point of the integration. The term P_n stands for the Legendre's polynomials ([43]).

The main problem with the solution of the equation 1.3 is that all the measurements are done on the topography surface or above it and the boundary surface is geoid. That requires reducing all the measurements down to the geoid level while using the approximate value of the orthometric heights. This process is called downward continuation and can be found in publications such as [44], [45], [46]. The disturbing potential must be a harmonic function outside the geoid (eq. 1.2), that means the measured gravity data must be corrected using the topographic corrections.

Converting the disturbing potential to geoid undulation is then given by equation

$$N(P_0) = T(P_0)/\gamma(Q_0). \quad (1.6)$$

1.4.1 Frequency components of the geoid

Since the disturbing potential T satisfies the Laplace's equation 1.2, T is a harmonic function. In that case it can be expressed in the form of an infinite harmonic series. In the spherical coordinates (r, ϕ, λ) it can be written as ([47])

$$T(r, \phi, \lambda) = \frac{GM}{R} \sum_{n=0}^{\infty} \left(\frac{R}{r} \right)^{n+1} T_n(\phi, \lambda), \quad (1.7)$$

⁶There is a unique solution in a form of the Green integral [40]. Green's integral theorems relate the gravitation potential of a continuous mass-density distribution in a limited area to integrals over the normal derivative of the potential and the potential itself at the boundary. That means the Earth's exterior gravitational potential can be calculated from observed data on the boundary.

⁷The symbol \iint_{Ω} is the usual abbreviation for an integral extended over the whole unit sphere $(\Omega_0) \rightarrow \Omega \subseteq \Omega_0$.

where T_n are Laplace's surface spherical harmonics ([47])

$$T_n(\phi, \lambda) = \sum_{m=0}^n [C_{n,m} \cos(m\lambda) + S_{n,m} \sin(m\lambda)] P_{n,m}(\sin \phi). \quad (1.8)$$

$P_{n,m}$ are Legendre's functions of degree n and m and $C_{n,m}$, $S_{n,m}$ are numerical spherical harmonic coefficients. Such approach is numerically very unstable since (from numerical stand point the coefficients usually underflow or overflow). And the practical applications are using fully normalized coefficients $\bar{C}_{n,m}$, $\bar{S}_{n,m}$ and fully-normalized associated Legendre's functions $\bar{P}_{n,m}$ ⁸ ([47], [49]).

1.4.2 Orthometric heights

The biggest problem of the rigorous definitions of the orthometric height is the evaluation of the mean value of the Earth's gravity acceleration along the plumbline between the level surface and the topography. To determine the orthometric height of an arbitrary point P above the level surface W_0 , based on the potential theory we use the equation ([47])

$$h_{ort}(P) = (W_0 - W(P))/\bar{g}, \quad (1.9)$$

where \bar{g} is the mean value of real gravity acceleration between the point P and level surface, measured along the real plumbline. The orthometric height can be computed from the geopotential number (eq. 1.9), if available. More practical approach is to compute it from spirit levelling measurements using the so-called orthometric correction, in which the mean value of gravity is embedded ([50]).

The main problem for the determination of orthometric heights is to develop a method for obtaining the mean gravity value. The first definition is attributed to Helmert ([51]). His definition of the orthometric height is based on Poincaré-Prey gravity gradient which is used to evaluate the approximate value of mean gravity from gravity observed on the Earth's surface. Later, the mean value of the gravimetric terrain correction inside the topography was taken into account ([52], [53]). More recently, the further corrections were introduced due to the vertical and horizontal variations in the topographical density ([54], [55] and [56]).

1.5 Detailed look at the Molodensky's problem

Because the Czech Republic and the Slovak Republic both use Molodensky's normal heights, the further look at Molodensky's problem is required. There are many ways how to approach this issue. Two basic concepts will be shown here. First one is related to the pre-GNSS era when measuring the ellipsoidal height directly was not possible. Instead, the normal heights obtained by geometric levelling played a huge role. In this case, the quasi-geoid is calculated using the free-air gravity anomalies.

Nowadays, when measuring the ellipsoidal height using GNSS technologies, it is not a problem any more. Hotine's solution is becoming quite common. This solution uses gravity disturbances instead of gravity anomalies.

1.5.1 Quasi-geoid

Since the Czech Republic and the Slovak Republic both use Molodensky's normal heights, the further look at Molodensky's problem is required. There are many ways how to approach this issue. Two basic concepts will be shown here. First one is related to the pre-GNSS era when measuring the ellipsoidal height directly was not possible. Instead, the normal heights obtained by geometric levelling played a huge role. In this case, the quasi-geoid is calculated using the Molodensky free-air gravity anomalies.

Nowadays, when measuring the ellipsoidal height using GNSS technologies, it is not a problem any more. Hotine's solution is becoming quite common. This solution uses gravity disturbances instead of gravity anomalies.

In the case of Molodensky's problem, the reference surface is not the geoid but the surface telluroid⁹. The biggest advantage of using the Molodensky's theory is that it can be solved without the proper knowledge of the topographic density distribution. This allows to avoid the necessity to extend the

⁸Which are solution of the Associated Legendre Differential Equation ([48])

⁹The telluroid (Σ) is used as an approximation to the Earth's surface ([57]).

gravity measurements from terrain down to geoid level. The telluroid is not a level surface because there is no constant value of geopotential. One of the possibilities of how to define the telluroid is through the gravity anomaly potential ([58])

$$\Delta W(P) = W(P) - U(Q), \quad (1.10)$$

where the gravity anomaly potential¹⁰ at P is given as a difference between gravity potential at that point $W(P)$ and normal potential at the point on telluroid's surface and lying on the vertical line passing the point P . The telluroid can also be defined by equation ([58])

$$\Delta \vec{g}(P) = \vec{g}(P) - \vec{\gamma}(Q), \quad (1.11)$$

where $\Delta \vec{g}$ is gravity anomaly vector. If the telluroid is defined by an appropriate way, it is possible to make one of the two anomalies equal zero. Because of this simplification compared to the Stokes' GBVP, equation 1.2 can be rewritten into

$$\left(\frac{\partial T}{\partial n_e} \right)_P - \frac{1}{\gamma_Q} \left(\frac{\partial \gamma}{\partial n_e} \right)_Q T(P) = -\Delta g(P) \quad \text{on } \partial\Omega = S_\Sigma, \quad (1.12)$$

where $\partial/\partial n_e$ is derivative in the direction of the vertical line to ellipsoid and boundary $\partial\Omega$ is Earth's surface.

The disturbing potential for Molodensky's problem is then given by

$$T(P) = \frac{\Delta GM}{r} + \frac{R}{4\pi} \iint_{\Omega} S(\psi_{P,\Omega}) \cdot (\Delta g(\Omega) + g_1(\Omega) + g_2(\Omega) + \dots) d\Omega \quad (1.13)$$

$$T(P) = \frac{\Delta GM}{r} + T_0(P) + T_1(P) + T_2(P) + \dots$$

Where Δg is free-air gravity anomaly, P is an arbitrary point on the Earth's surface and terms g_i are members of the Molodensky's series and will be discussed in the following section 1.5.2. The relation between the ellipsoidal heights h_{el} and Molodensky's normal heights h_n is given by following equation

$$h_{el} = h_n + \zeta, \quad (1.14)$$

where ζ is height anomaly representing the vertical difference between topography and telluroid at point P

$$\zeta(P) = T(P)/\gamma(Q) \quad (1.15)$$

1.5.2 Molodensky's problem - free boundary value problem

Using the gravity anomalies to determine the physical surface of the Earth is known as Molodensky's problem. The surface gravity anomalies are linear functions of the harmonic potential outside the Earth masses and so they can not be directly used in Stokes' integral (see eq. 1.3). This is because they are related to the physical surface, which can not be considered as the equipotential surface of the gravity field. Isozenithal¹¹ lines are not in general perpendicular to telluroid, that resolves into solving the linear boundary problem with oblique derivation (see for example [60], [61]). The spherical approximation of the equation 1.12 with the use of Marussi telluroid ($\Delta W = 0$) is

$$\Delta g(P) = \frac{2T(P)}{r} - \left(\frac{\partial T}{\partial r} \right)_P \quad \text{on } \partial\Omega = S_\Sigma, \quad (1.16)$$

The classical solution is often marked as Simple Molodensky's problem (SMP) because it uses the expansion into infinite series (see eq. 1.13). In the case where only the first two members of the infinite series are used, it is called the gradient solution. This approach uses the free-air gravity anomalies Δg_{FA}

$$g_0(P) = \Delta g_{FA}(P), \quad (1.17)$$

¹⁰For example the commonly used Marussi telluroid is defined by condition $\Delta W(P) = 0$.

¹¹Isozenithal of the normal gravity field is a line on which all the gravity vectors parallel to themselves, for isozenithal lines related to Molodensky's problem see [59])

$$g_1(P) = R^2 \iint_{\Omega} \frac{h_n(\Omega) - h_n(P)}{l_0^3(P, \Omega)} \left(\Delta g_{FA}(\Omega) + \frac{3T_0(\Omega)}{2R} \right) d\Omega, \quad (1.18)$$

where h_n and $h_n(P)$ stand for Molodensky's normal heights of the integration point and computation point P . The T_0 is initial approximation of the disturbing potential¹². And $l_0(P, \Omega)$ is given by equation

$$l_0(P, \Omega) = 2R \sin \frac{\psi_{P, \Omega}}{2}. \quad (1.19)$$

Listed formulas (published in [62]) show that instead of a straightforward integration of the Δg_{FA} , the iterative process is required. This process also involves height differences between the running point of the integration and the rest of the points on the terrain. In Molodensky's theory, the height anomaly ζ can be expressed as infinite series ([63]):

$$\zeta = \zeta_0 + \zeta_1 + \zeta_2 + \dots + \zeta_n, n \in \mathbb{N}. \quad (1.20)$$

In many practical applications, only the first two terms are needed. The higher terms are necessary only in mountainous areas. In paper [64] the use of Molodensky series up to 3^{rd} order is studied for a mountainous Alps region located near Mount Blanc. The contribution of ζ_1 reaches maximum values up to 0.10 m, ζ_2 contributes up to 0.01 m and the contribution of ζ_3 is practically negligible. It is also important to mention that the Molodensky series converges only when the terrain inclination is less than 45° ([65]). That means that when using very high-resolution DEMs it can cause some numerical instabilities.

1.5.3 Molodensky's problem - fixed boundary value problem

The most common computation method for the quasi-geoid calculation is so-called remove-restore technique ([66]). With the development of the GNSS technology and other advanced remote sensing technologies, the Earth's surface can be observed with few centimetres accuracy. The conclusion of this technology development is that the Earth's surface can be considered as given. The usage of the telluroid as a reference surface is still necessary. This problem is called the fixed GBVP and has been investigated in many publications [67], [68], [69].

When the Earth's surface is considered as the boundary and the gravity disturbance δg is given on that boundary, assuming that no masses are outside the Earth, then for the relation between disturbing potential T and δg under linearisation and spherical approximation the following equation is given

$$\delta g = - \left. \frac{\partial T}{\partial h} \right|_S \quad \text{on the Earth's surface } S, \quad (1.21)$$

also two other conditions must be fulfilled

$$\begin{aligned} \nabla^2 T &= 0 \quad \text{on and outside of } S, \\ \lim_{\|r\| \rightarrow \infty} T(\vec{r}) &= 0. \end{aligned} \quad (1.22)$$

The equations in 1.21 and 1.22 are formulation of the Neumann's boundary value problem. To avoid the density hypothesis, the Molodensky's solution for the equation 1.21 is given by

$$T(P) = T_0(P) + T_1(P) = \frac{R}{4\pi} \iint_{\Omega} \delta g(\Omega) H(\psi_{P, \Omega}) d\Omega + \frac{R}{4\pi} \iint_{\Omega} \delta g_1(\Omega) H(\psi_{P, \Omega}) d\Omega, \quad (1.23)$$

where $H(\psi)$ is the Hotine's function [70] in closed form

$$H(\psi) = \frac{1}{\sin \frac{\psi}{2}} - \ln \left(1 + \frac{1}{\sin \frac{\psi}{2}} \right), \quad (1.24)$$

¹²reminder: $\zeta_0(P) = T_0$

or it can be expressed in form of the infinite series - spectral form ([41])

$$H(\psi) = \sum_{n=0}^{\infty} \frac{2n+1}{n+1} P_n(\cos \psi), \quad (1.25)$$

Analogously to the previous chapter where the free boundary problem was discussed the terms δg_i are the terms of the Molodensky series. The first term is given by

$$\delta g_1(P) = \frac{R^2}{2\pi} \iint_{\Omega} \frac{h_{el}(\Omega) - h_{el}(P)}{l_0^3(P, \Omega)} \left[\delta g(\Omega) - \frac{1}{8\pi} \iint_{\Omega} \delta g(\Omega) H(\psi) d\Omega \right] d\Omega. \quad (1.26)$$

This solution is explained further in [71].

However, the lacking availability of globally distributed δg can create some complications. Since the majority of available gravity measurements are from pre-GNSS era, when the ellipsoidal heights have not been determined.

The gravity disturbances can not be compiled, since the gravity measurements have been used to compute the gravity anomalies and the original data are almost impossible to obtain. In the article [72], the effect of local datum offset on gravity anomalies is mentioned and the relation between the δg and Δg is discussed to a large extent.

1.6 Computing the connection between Local Vertical Datum and Global Vertical Reference Frame

Due to the high count of the local vertical datums, the Earth's surface is partitioned into n disjoint zones Λ^i , $i = 1, 2, \dots, n$. Important to mention is also that there is no intersection¹³ of these datum zones Λ^i . It means that $\Sigma = \cup_{i=1}^n \Lambda^i$ while $\Lambda^i \cap \Lambda^j = \emptyset$ for every $i \neq j$. The "origin" of each datum zone is defined by its own level surface, e.g. the gravity potential value $W_{0,i}$. Such case is displayed in the figure 1.2.

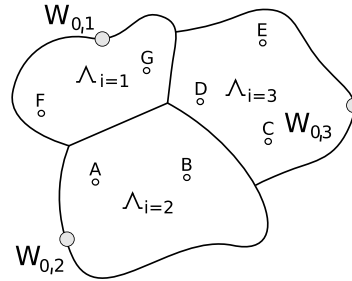


Fig. 1.2: Schema of the disjoint vertical datums. Each VD has its origin $W_{0,i}$ and a set of GNSS/levelling points distributed over the territory [author].

For these GNSS/levelling sites, the ellipsoidal heights $h_{el,i}$ are unbiased and normal heights h_n are biased. For these benchmarks, the biased height anomaly ζ_i can be linked to the disturbing potential T by the generalized Brun's formula ([73]):

$$\zeta_i(P) = \frac{T^i(P) - (W_{0,i} - U_0)}{\gamma(Q_i)} = \frac{T(P) + \Delta W_0}{\gamma(Q_i)}, \quad (1.27)$$

where U_0 stands for the constant normal gravity potential value on the surface of the reference ellipsoid, γ is the normal gravity value at the Earth's surface and $\Delta W_0 = W_0 - U_0$. The $\delta W_{0,i} = W_{0,i} - W_0$. Inserting last two terms into equation 1.27 we get

$$\zeta_i(P) = \frac{T^i(P) - \Delta W_0}{\gamma(Q_i)} - \frac{\delta W_{0,i}}{\gamma(Q_i)}, \quad (1.28)$$

¹³Common boundary is allowed.

where the last term is the unknown height datum offset of the i -th LVD. The disturbing potential can be obtained from solving boundary value problem based on the gravity disturbance (section 1.5.3 Molodensky's problem - fixed boundary value problem) or based on free-air gravity anomalies (section 1.5.2 Molodensky's problem - free boundary value problem).

Let us consider the Global Vertical Reference System and the $\zeta(P)$ is given in the same way as $\zeta^i(P)$, the unknown height offset correction is given by

$$\Delta\zeta^i = \zeta(P) - \zeta^i(P) \quad (1.29)$$

Since the $\zeta^i(P)$ is given as a official reference surface used in the i -th country it is the $\zeta(P)$ that needs to be determined using the fixed-GBVP.

1.7 'FAST' GBVP connection to WHS

Since the territories of the Czech Republic and the Slovak Republic use Molodensky's concept of normal heights, they will be discussed more thoroughly. For normal heights based on Molodensky's theory, the equation 1.9 is rewritten into

$$h_n(P) = (W_0 - W(P))/\bar{\gamma}, \quad (1.30)$$

where $\bar{\gamma}$ is mean value of the normal gravity measured along the normal vertical between the point P and level surface represented by level ellipsoid E_0 (see equation 1.41) where $W_{0,i}$ is the value of gravity potential at the i -th tide gauge station. That means that different tide gauges have difference value of gravity potential and in general they are not at the same equipotential surface.

The FAST GBVP connection is based on method previously developed for testing the geopotential models ([1], [74]). The difference between the normal gravity potential and the real one is directly related to the ζ value and then, of course, also to the h_n value. So the practical realisation of GVRS can be derived from the following equations. Let the W_0 represent the GVRS and $W_{0,i}$ the LVD. And let

$$U_0 = W_0 \neq W_{0,i}, \quad (1.31)$$

The value W_0 is well known and the $W_{0,i}$ is the value to be determined. At point Q_i the normal potential is equal to gravity potential at point P .

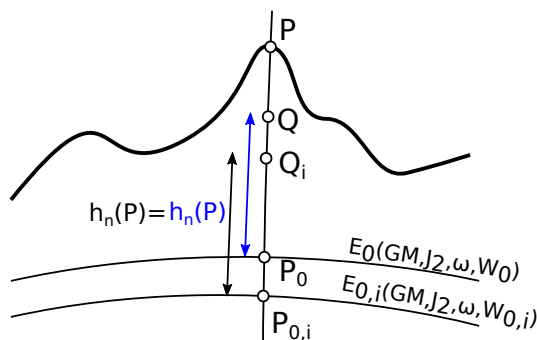


Fig. 1.3: The difference between LVD and GVRs [author].

$$U(Q_i) = W(P). \quad (1.32)$$

The spatial position of Q_i is defined by normal Molodensky's height. But at Q

$$U(Q) \neq W(P), \quad (1.33)$$

because the spatial position of this point is related to different ellipsoid E_0 . In that case

$$U(Q) - U_0 = U(Q_i) - U_{0,i} \quad \text{or} \quad U(Q) - W_0 = W(P) - W_{0,i}, \quad (1.34)$$

that means that the normal height is identical in both cases. The offset between W_0 and $W_{0,i}$ is then given by

$$U(Q) - W(P) = W_0 - W_{0,i} = -\delta W_{0,i}. \quad (1.35)$$

The last equation defines the difference between the LVD and GVRS. This methodology for geopotential model testing was developed by [1]. As a by-product of testing geopotential models, the technology was developed for determining the geopotential values at the tide gauge stations, which are used for specifying the LVDs over areas covered by GNSS/levelling sites ([3]). This technology is based on boundary condition defined by the equation 1.10. The final equation is then given by

$$\delta W_{0,i} = W(P) - U(Q). \quad (1.36)$$

The $W(P)$ can be obtained either from GGFM model or by converting the normal height to geopotential number using equation 1.30.

In modern world this information can be measured by GNSS technologies (coordinates of the point P). The second member of the mathematical statement $U(Q)$ in equation 1.36 is computed based on Molodensky's theory using the level ellipsoid and normal height, thus

$$U(Q) = U(E_0(GM, \omega, J_{20}, W_0), H_n) \quad \text{or} \quad U(Q_i) = U(E_{0,i}(GM, \omega, J_{20}, W_{0,i}), H_n), \quad (1.37)$$

if the use of different $W_{0,i}$ is required. The computation of the normal potential can be done using the equations published in [75], [76]. But for numerical computations done for the purpose of this doctoral thesis the curvilinear coordinates were used [77]. The radial distortion δR of the LVD is then given by equation

$$\delta R = -\frac{GM}{(W_{0,i})^2} \cdot \delta W_{0,i}. \quad (1.38)$$

1.7.1 The definition of the level ellipsoid

In order to connect the GGFM with the geopotential value on the level surface of the geoid (W_0), it is necessary to calculate the parameters of the level ellipsoid E_0 . The level ellipsoid has the same potential value on its surface as the geoid.

The computation can be performed using following equations ([15]):

$$\begin{aligned} f_{i+1} &= \frac{f_i^2}{2} + \frac{3}{2} \left(\frac{a_0}{a_i}\right)^2 J_{20} + \frac{2}{15} q \left(\frac{a_i}{a_0}\right)^3 e_i^{3/2} \cdot \left[\frac{3-2e_i^2}{e_i^2} \cdot \arctan \sqrt{\frac{e_i^2}{1-f_i}} \right]^{-1}, \\ a_{i+1} &= \frac{GM}{W_0} \cdot \frac{1}{e_i} \arctan \left(\frac{e_i}{1-f_i} \right) + \frac{1}{3} \omega^2 a_i, \end{aligned} \quad (1.39)$$

where a_0 is reference radius of the used GGFM, $J_{2,0}$ is derived from GGFM coefficients using equation $J_{2,0} = -\sqrt{5}C_{2,0}$, W_0 is value of the geopotential on the geoid surface, ω is angular velocity of the Earth's body, e is first numerical eccentricity.

In order to check if the computed level ellipsoid has the same geopotential value on its surface as geoid, the following equation can be used :

$$\bar{W}_0 = \frac{GM}{ae} \arctan \left(\frac{e}{1-f} \right) + \frac{1}{3} \omega^2 a^2, \quad (1.40)$$

Such defined level ellipsoid can be expressed as function of four fundamental constants used in geodesy. For a general value of $W_{0,i}$ the level ellipsoid $E_{0,i}$ is given by equation

$$E_{0,i} = E_{0,i}(GM, \omega, J_{20}, W_{0,i}). \quad (1.41)$$

In the table 1.2 the parameters for the level ellipsoids are shown. The computation used the same value for GM , ω and $W_{0,i}$. The value C_{20} however changes for different tide systems.

Tab. 1.2: Parameters of the level ellipsoids using the C_{20} from EGM08 model, $GM = 3.986004415 \cdot 10^{14} \text{ m}^3 \text{ s}^{-2}$, $\omega = 7.292115 \cdot 10^{-5} \text{ rad} \cdot \text{s}^{-1}$. The values are listed for the different values of W_0 and for all three permanent tide systems [author].

Permanent Tide System	Parameters	Geopotential value W_0 [$\text{m}^2 \text{s}^{-2}$]	
		62635856.0	62635853.4
Tide Free	a-axis [m]	6378136.545	6378136.810
	b-axis [m]	6356751.898	6356752.163
	f^{-1} [dimensionless]	298.257755	298.257748
	$C_{20} \cdot 10^{-4}$ [dimensionless]	-4.841651	-4.841651
	γ_e [ms^{-2}]	9.738129	9.738129
	γ_p [ms^{-2}]	9.836951	9.836950
Mean Tide	a-axis [m]	6378136.415	6378136.681
	b-axis [m]	6356752.156	6356752.420
	f^{-1} [dimensionless]	298.263141	298.256520
	$C_{20} \cdot 10^{-4}$ [dimensionless]	-4,841471	-4,841471
	γ_e [ms^{-2}]	9.738130	9.738129
	γ_p [ms^{-2}]	9.836950	9.836950
Zero Tide	a-axis [m]	6378136.574	6378136.840
	b-axis [m]	6356751.840	6356752.104
	f^{-1} [dimensionless]	298.256527	298.256520
	$C_{20} \cdot 10^{-4}$ [dimensionless]	-4.841693	-4.841693
	γ_e [ms^{-2}]	9.738129	9.738129
	γ_p [ms^{-2}]	9.836951	9.836950

1.7.2 The permanent tide role in height systems and transformation between them

The treatment of the permanent tidal deformation of the Earth's crust plays an important role in the realisation of the height system and also in GNSS positioning. With modern possibilities and increasing precision of GNSS based coordinates, all methods of the height system unification require precise and consistent way how to handle the tides. Different concepts of how to handle these deformations are described in [78], [79], [80].

The tides are generated by external bodies: the Moon and the Sun. Their gravity generates forces that deform the shape of the Earth. The tidal deformations are usually divided into two groups: permanent (time-independent part) and periodic.

A **tide-free (TF)** (or non-tidal) system eliminates the permanent deformation from the shape of the Earth. Both parts, the tide generating potential and the deformation potential of the Earth (the indirect effect), are eliminated from the potential field quantities (such as gravity, geoid, potential, etc.). Thought experiment behind is that the external bodies such as the Sun and the Moon are physically moved to infinity. That means the Earth is rid of all direct and indirect effects of the Sun and the Moon. Typically the permanent deformation is treated using the Love numbers h and k , and the Shida number l .

The tide-free gravity field and Earth's crust do not compare with the real Earth and gravity quantities are not directly observable (see [81], [82]).

A **mean-tide (MT)** system does not remove the permanent effect from the Earth's shape. The shape corresponds to the long-time average under tidal forcing. The potential field preserves the potential of time-average shaped Earth. Mean-tide potential field basically characterizes how water flows and clocks run according to Einstein general relativity ([83]).

A **zero-tide (ZT)** potential is generally a *middle alternative* for treating the tidal deformations. It eliminates the tide generating potential but possesses its indirect effect (effect mostly related to

the elasticity of the Earth is retained). The gravity field is generated only by Earth's mass plus the centrifugal force.

The permanent tide in height systems can not be considered separately from the permanent tide in other geodetic and gravity quantities. The IAG Resolution Number 16 adopted in 1983 at the General Assembly in Hamburg ([84]) states that: that the indirect effect due to the permanent yielding of the Earth should be not removed.

Once the height of an arbitrary point is acquired, the tidal transformation equations can be expressed in following way. In case of the transformation of the heights, the following equations are used:

$$\begin{aligned} H^{MT} &= H^{TF} - (1 + k + h) \cdot \Delta W^{ZT} \cdot g^{-1} \\ H^{ZT} &= H^{TF} - (k - h) \cdot \Delta W^{ZT} \cdot g^{-1} \\ H^{MT} &= H^{ZT} - \Delta W^{ZT} \cdot g^{-1}, \end{aligned} \quad (1.42)$$

where k and h are the tidal Love numbers. The term $\Delta W \cdot g^{-1}$ in equations 1.42 can be calculated with sub-centimetre accuracy using the following expression ([85]):

$$\frac{\Delta W^{ZT}}{g} \approx -0.198 P_{2,0}(\sin \phi) [\text{m}] = -0.198 \left(\frac{3}{2} \sin^2 \phi - \frac{1}{2} \right) [\text{m}]. \quad (1.43)$$

1.8 Residual terrain modelling

As it was mentioned before, many GGFM do not contain the high-frequency content of the gravitation field. The high frequencies are generated mostly by the terrain near the evaluation point. The gravity quantity can be evaluated separately using the DEM and then added to the reference part of the signal computed from GGFM. This combination of data was chosen in order to calculate the connection between the local height system and the WHS because of the lack of well-distributed quality gravity data. Then the gravity anomaly Δg can be expressed as

$$\Delta g(P) \approx \Delta g(P)^{GGFM} + \Delta g(P)^{RTM}, \quad (1.44)$$

where $\Delta g(P)^{GGFM}$ stands for the gravity anomaly obtained from GGFM at an arbitrary point P and $\Delta g(P)^{RTM}$ is the residual terrain part of the gravity anomaly computed from DEM. The error of the approximation of the true gravity anomaly acquired by combining the GGFM with RTM technique is given by equation:

$$\Delta g \approx \Delta \tilde{g} \rightarrow \Delta g^\epsilon = \Delta g - \Delta g^{GGFM} - \Delta g^{RTM}. \quad (1.45)$$

According to the [86], the error of the approximation is mainly effected by:

- commission error of the $\Delta g(P)^{GGFM}$ (caused by errors in GGFM coefficients),
- errors in $\Delta g(P)^{RTM}$ (caused by limited knowledge of the density inside, the Earth's topography, precision of DEM and used method of the evaluation),
- non-seamless spectral separation of two terms in equation 1.44,
- missing higher frequencies (caused by limited resolution of the DEM),
- errors in upward or downward continuation of the Δg between the mean surface and the real topography.

The main problem with the RTM is the fact that the gravitational signal of the topography contributes to all frequencies of the gravitation potential. That means that it contributes also to the frequencies that are already included in GGFM. For example the EGM08 or EIGEN-6C4 already contain the gravity signal contribution of the world topography. For the spectral combination of Δg^{GGFM} and Δg^{RTM} , only the Δg^{RTM} frequencies that are higher than the maximal frequency of GGFM should be considered.

1.9 Gravity field modelling

The gravity field modelling using tesseroids ([87]) is being used for calculation of the gravity quantities from DEMs. Residual terrain modelling (RTM) is a technique that allows forward modelling of the high-frequency gravity effects from the topographic mass ([66]).

Since the shape of the Earth's body is well known today due to the development in creation of DEMs and methods of collecting data, it is possible to compute the contribution of the topographic masses to gravity data such as gravity disturbance or gravity anomaly and many others. Forward gravity field modelling (FGFM) is based on well known Newton's integral for gravitational potential of a solid body $\sigma \in \mathbb{R}^3$:

$$V(P) = G \iiint_{\sigma} \frac{\rho(\sigma)}{l(P, \sigma)} d\sigma, \quad (1.46)$$

where G denotes Newton's gravity constant, $\rho(\sigma)$ is density function, $l = l(P, \sigma)$ is Euclidean distance between the attracted computation point $P \in \mathbb{R}^3$ and the running mass point $Q \in \sigma$. By solving the equation 1.46, we can obtain the value of gravitational potential of surrounding terrain. Applying the Leibniz integral rule, the other parameters of a gravity field, such as first and second derivatives of a gravitational potential, can be obtained respecting the chosen coordinate system.

Modern way how to treat with contribution of topographic masses to gravity based values (potential and its derivatives) is the usage of tesseroid geometry. Let's have point $P(r, \varphi, \lambda)$ for which the values are computed. Each tesseroid is given as a volume with following boundaries $\sigma = [r_1, r_2] \times [\varphi_1, \varphi_2] \times [\lambda_1, \lambda_2] \in \mathbb{R}^3$. Also the required condition is $P \notin \sigma$, but it can be part of the tesseroid's boundary $P \in \partial\sigma$, and an arbitrary point $Q \in \sigma$ has coordinates (r', φ', λ') . The geometry of spherical tesseroids and its solution is published in [88]. Optimized tesseroid formulas based on Cartesian integral kernels were introduced in [87].

The RTM techniques can be used in context of smoothing the gravity field observations, for example, the remove-restore gravity field computations ([89]) or determining the high frequency geoid models ([90]). Another application of RTM techniques can be the extension of the spectral content of GGFMs to the short-wave length domain not originally included in GGFMs (e.g [91]). The spectral enhancement method can be also used to fill the spectral gap between the spherical harmonics models and gravity field observations (for example the deflections of the vertical [92], GNSS/levelling [93], etc.) Possible applications are also predicting the values of gravity field quantities ([94]) or for the purpose of this doctoral thesis, the height system unification ([95]).

Using the RTM for high-frequency GGFM augmentation, spectral inconsistencies can resolve into errors. The spectral inconsistencies can be reduced by using a spherical harmonic reference surface ([91]) which is related or obtained directly from DEM data itself via spherical harmonics analysis ([96]). However, the calculated RTM gravity effects are related to approximation errors, because filtering in the topography and in gravity domains are not equivalent operations (known as RTM filter problems).

1.9.1 Terrain effects

The terrain effect (TE) is an effect of the physical terrain on the gravitational potential of the planet's body or its other derivatives. The definition of the terrain can be defined as the part of the topography which rises above or below the local horizon of an arbitrary point P located on the planet's surface. The surface of the Earth is best represented by DEM. DEM can be provided in various forms.

Height in those models can be given above different surfaces such as geoid (orthometric heights), quasi-geoid (normal heights) or reference ellipsoid (ellipsoidal heights). Because of the fact that the terrain is characterized by relative elevation of the topography with respect to an arbitrary point P and also most of the computations of TE are done up to a maximum distance of tens of arc minutes, or maximally up to one degree, the differences between various types of heights using the spherical approximation can be neglected.

1.10 Mean elevation surface

The main thought behind the combination of DEM with GGFM is adding the topography to gravity quantities calculated from geopotential models. The merge is done by using a mean elevation surface (MES) that corresponds to given GGFM, i.e. has the same spatial resolution. MES helps to distinguish the signals that are already a part of GGFM from the signals generated by the best available DEM. MES can be given in various forms, but from frequency point of view, the spherical harmonics expansion of the global topography to the same degree and order as GGFM is the most suitable format.

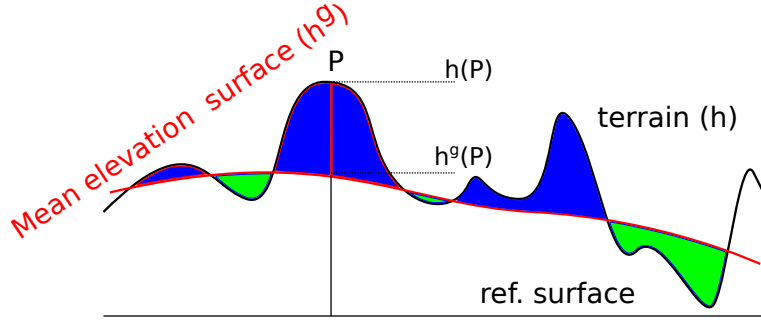


Fig. 1.4: The comparison of mean elevation surface and real topography. The residual terrain effect is also shown on the picture [author].

The main difference between the classic terrain correction (CTC) and TE is that the CTC represents the gravitational effect of topography masses between a constant elevation level of an arbitrary point P and the topographical surface, while TE represents the gravitational effect of masses between MES and actual topography.

On figure 1.4 the RTM anomalies are shown. They consist mostly of balance set of positive and negative density anomalies, representing the areas where the topography is either above or below the MES. Hence the gravitational effect of the RTM will in general cancel out in larger distances from a computational point (in [86] distance of 2-3 times the of the MES resolution is mentioned).

However, there are two important aspects of RTM. The first one is the harmonic correction. The second variable is large effect generated by the unlimited Bouguer layers.

1.10.1 Harmonic correction

The gravitational effect, in this case, is modelled by using the spherical (or planar) approximation. The bottom edge of the prism has an elevation of $h^g(P)$ and the height at the top edge has the value $h(P)$. The harmonic correction (HC) deals with the case where $h(P) < h^g(P)$. In that case, it is necessary to evaluate an arbitrary point P inside the MES. That situation is not automatically managed by the forward gravity field modelling methods and so the correction known as harmonic correction has to be taken into account. This problem was mentioned for the first time in [97]. In this paper, the harmonic correction was developed only for gravity anomaly, therefore no other harmonic corrections for other gravity quantities were introduced. That problem was mentioned multiple times in papers such as [98] or [99]. Omang et al. proposed the approach where the P is moved above the MES, then the topography is removed and the final step is to analytically continue the calculated value back to the original point P below MES. In paper [66], the conventional solution to harmonic correction is expressed as

$$HC \approx \begin{cases} 4\pi G\rho h^{RTM}(P), & h^{RTM}(P) < 0 \\ 0, & \text{otherwise} \end{cases} \quad (1.47)$$

where $h^{RTM}(P)$ is defined as $h^{RTM}(P) = h(P) - h^g(P)$.

The HC relies on a mass condensation based on a double Bouguer reduction with slab thickness $h^{RTM}(P)$. The value of $h^{RTM}(P)$ has oscillating nature. The gravity anomaly from RTM in the spherical coordinates is given by equation:

$$\Delta g^{RTM} \approx HC + G\rho \int_0^{\psi_0} \int_0^{2\pi} \int_{R+h^g(P)}^{R+h(P)} \frac{(r')^2 \cdot (r - r' \cos \psi')}{l^3} dr' d\alpha' \sin \psi' d\psi', \quad (1.48)$$

where R is the radius of the reference sphere, α is azimuth and ψ is geocentric angle.

The harmonic correction has its place in cases when the available model is capable to model gravity outside masses as a harmonic function and inside masses as a non-harmonic function. The GGFMs which are expressed as a series of spherical harmonics are not capable of handling the non-harmonic functions. That means that the values obtained from GGFMs above the reference ellipsoid

act as harmonic functions. That applies also for points which are in reality inside the masses. The non-harmonicity of functions inside masses is not part of GGFM and should not be corrected.

1.11 Remove-Compute-Restore Technique

To avoid the numerical integration around the whole globe, the Remove-Compute-Restore (RCR) technique is used ([62]) to determine the quasi-geoid with an accuracy on the cm level which matches the accuracy of GNSS heights. In this thesis, the disturbing potential is computed using the convolution technique for fast approach. The RCR method removes from the measured data the long-wavelength component (predicted by GGFM) and a short-wavelength part (predicted by topography). Both parts are removed from the original gravity data. Then the remaining wavelength part of the signal is transformed into the height anomaly representing the quasi-geoid. This step is carried out either using the Hotine's or Stokes' integral or using the Least Squares Collocation (LSC). After this step, the signals originally removed from the data are restored. The advantage of the LCS over the Stokes'/Hotine's integral is that it does not require the gridded gravity anomalies as the FFT approach of the mentioned integrals do. Also, the LSC provides the error estimation for the resulting quasi-geoid models.

Since the real gravity data are not easily obtainable, the modification of the RCR method was used. For these calculations, the GGFM model with a combination of the DEM representing the topography was used. For example, the integration radius was set to $1.1^\circ \approx 122$ km. The signal representing the global contribution is the value computed only from the coefficients of the GGFM up to degree and order 164. From degree and order 165 to the maximum possible degree and order, the values represent the gravity signal which is then integrated. The remaining high frequencies which are not included in GGFM are added via residual terrain modelling (RTM, see section 1.8 Residual terrain modelling), are integrated accordingly to their spatial resolution.

It is important to mention that using the full form of the integral kernels is legitimate when the $\Delta g/\delta g$ contain all the frequencies. Otherwise the spectral form of this functions is needed. In case, when the frequencies from degree and order 165 up to 2190 are used the spectral form of the integral kernel. For the Stokes' kernel we assume the bandwidth $n = 165 \dots 2190$ in equation 1.5. So the notation $S_l^u(\psi)$ is used for bandwidth limited kernel. The Hotine's kernel can be defined analogously.

The final value of the disturbing potential using GGFM such as EIGEN-6C4 or EGM08 can be expressed in the following form using the Stokes' integral:

$$\begin{aligned} T &= T^{GGFM_0^{164}} + \frac{R}{4\pi} \iint_{\Omega} (\Delta g^{GGFM_{165}^{2190}} + g_1^{GGFM_{165}^{2190}}) S_{165}^{2190}(\psi) d\Omega \\ &+ \frac{R}{4\pi} \iint_{\Omega} (\Delta g^{RTM} + g_1^{RTM})(S(\psi) - S_{165}^{2190}(\psi) - S_2^{164}(\psi)) d\Omega, \end{aligned} \quad (1.49)$$

or the Hotine's integral:

$$\begin{aligned} T &= T^{GGFM_0^{164}} + \frac{R}{4\pi} \iint_{\Omega} (\delta g^{GGFM_{165}^{2190}} + \delta g_1^{GGFM_{165}^{2190}}) H_{165}^{2190}(\psi) d\Omega \\ &+ \frac{R}{4\pi} \iint_{\Omega} (\delta g^{RTM} + \delta g_1^{RTM})(H(\psi) - H_{165}^{2190}(\psi) - H_0^{164}(\psi)) d\Omega. \end{aligned} \quad (1.50)$$

Since for the RTM obtained values it is quite hard to determine the frequency numbers, the remaining value of the kernels is used ($\bar{H}(\psi) = H(\psi) - H_l^u(\psi)$).

2 THE CASE STUDY FOR THE TERRITORIES OF THE CZECH REPUBLIC AND THE SLOVAK REPUBLIC

2.1 Input data

The data used for the Vertical Reference Frame connection to the WHS were the DEM GMTED10 [14], which is freely available, and different GGFMs namely EIGEN-6C4, EGM08 and XGM2019e. For the results verification, the points from the territories of the Czech Republic and the Slovak Republic with known ellipsoidal heights and also the normal Molodensky's heights were used. The number of points differs for both countries. For the territory of the Slovak Republic, the total number of points is 5614 and for the territory of the Czech Republic, it is 2430. For every j -th GNSS/levelling point the gravity potential $W(P_j)$ and normal potential using the level ellipsoid for corresponding point on the telluroid surface $U(Q_j)$ is computed. The difference between these values is converted from geopotential numbers to SI scale unit-m, using the γ value. Some of these points were rejected in the adjustment process as the error exceeding the condition $|v| \geq 3 \cdot \sigma_0$, where the σ_0 is a posteriori standard deviation and v is error value. Such values are considered to be remote and are removed from the process.

When the FAST GBVP approach was computed, 10% of all points were reserved to verify the results, thus they were not used in the adjustment process.

The GNSS/levelling data from the territory of the Czech Republic are so called Points of Selected Maintenance¹, these points have their heights measured by GNSS technologies and also by spirit levelling. They were primarily used for creating the National coordinate reference frame *Jednotná trigonometrická síť katastrální*² (S-JTSK). One downside is the fact that spirit levelling, in this case, is mostly done only by technical levelling. The kilometre error in millimetres for such levelling line is $20 \cdot \sqrt{R}$ [km], where R is the length of the levelling line in kilometres. The geodetic coordinates are determined in ETRS89 coordinate system by static method with length of observation of 3 hours or longer. The expected precision in ellipsoidal height is around a few centimetres.

The GNSS/levelling points from the territory of the Slovak Republic are mostly points of the high precise levelling lines, so their normal heights are measured in millimetre precision, but their ellipsoidal heights are often measured by GNSS-RTK method. Expected height precision is around $\pm 3 - 4$ cm.

The digital elevation model GMTED10 is an enhanced global DEM developed by the U.S. Geological Survey (USGS) and the National Geospatial-Intelligence Agency (NGA) which replaces the DEM GTOPO30. For all the computations the 7.5'' resolution was used since the Europe coverage is provided in high resolution. For the latitude of the Czech Republic the grid resolution is approximately 225 [m] \times 150 [m].

2.2 Adjustment process

The results obtained from previously discussed methods (see section 1.7 'FAST' GBVP connection to WHS and section 1.6 Computing the connection between Local Vertical Datum and Global Vertical Reference Frame) were processed using the equation 2.1.

$$\Delta\zeta_i + v_i = \delta R + a \cdot (\varphi_i - \varphi_0)M + b \cdot (\lambda_i - \lambda_0)N \cos \varphi_0, \quad (2.1)$$

where $\Delta\zeta$ is difference between the local quasi-geoid and the quasi-geoid describing the WHS, v_i is residual value, δR is vertical offset of the local datum, a is tilt of the local geodetic datum in *north-south* direction and b is tilt in *west-east* direction, φ_0 , λ_0 is the origin of the local coordinate system in latitude direction, longitude direction, M is meridional radius for φ_0 , N is radius of curvature in the prime vertical for φ_0 . The unknown variables in this equation are δR , a , b . By using the Least

¹In Czech language: Body výběrové údržby.

²Translation: Datum of Uniform Trigonometric Cadastral Network

Square Adjustment the design matrix for the projection between the measured quantities and the unknown parameters is:

$$A = \begin{bmatrix} 1 & (\varphi_1 - \varphi_0)M & (\lambda_1 - \lambda_0)N \cos \varphi_0 \\ 1 & (\varphi_2 - \varphi_0)M & (\lambda_2 - \lambda_0)N \cos \varphi_0 \\ \vdots & \vdots & \vdots \\ 1 & (\varphi_1 - \varphi_0)M & (\lambda_1 - \lambda_0)N \cos \varphi_0 \end{bmatrix} \quad (2.2)$$

and the unknown parameters are then given by:

$$\delta\vec{x} = (A^T Q_{ll}^{-1} A)^{-1} A^T Q_{ll}^{-1} \Delta\vec{\zeta} = N^{-1} A^T Q_{ll}^{-1} \Delta\vec{\zeta}, \quad (2.3)$$

where Q_{ll} is the covariance matrix of measured parameters. The order of estimated variables in vector $\delta\vec{x}$ is δR , a and b . The estimates for the standard deviations of the unknown parameters are computed and multiplied by the square of unit a posteriori standard deviation.

$$\Sigma_{xx} = \sigma_0^2 N^{-1} \quad \text{where} \quad \sigma_0^2 = \frac{\sum_{i=0}^n v_i^2}{n - k}. \quad (2.4)$$

The n is number of observed parameters, k is number of unknown parameters.

The members of the main diagonal of the Σ_{xx} matrix are estimates of standard deviation for unknown parameters (in order $\sigma_{\delta R}^2$, σ_a^2 , σ_b^2). In the tables which are summarizing the results, the values are listed under *STD* columns.

2.3 Results by FAST GBVP

The method called FAST GBVP in this doctoral thesis as FAST GBVP was applied to the territories of the Czechia and the Slovakia which both are using the Kronstad Height Datum (KHD)³. Various GGFMs were used and the adjustment process was applied to each country separately and also using all available data. The reference value W_0 was set to either value 62 636 586.0 [m²s⁻²] or 62 636 583.4 [m²s⁻²]. The summary of these calculations is in table 2.1. The constants of tilt a and b from equation 2.1 were transformed into format m/100 km, since the original values were in magnitude of 10⁻⁸.

The results clearly show that the value of chosen W_0 has practically no impact on the solution in case of precision or tilt values, except for the difference in the value of the datum shift δR . The vertical shifts of LVDs when treating both territories separately are very similar, they differ only by a couple of millimetres when using the same GGFMs. Interestingly, the tilt values a and b for both territories differ quite much. For example, using the GGFMs EGM08, the $[a, b]$ values for Czechia are $[-0.0098, +0.0019]$ and for Slovakia $[+0.0321, -0.0088]$, all dimensions for values a, b are in m/100 km. A possible explanation for this fact may be that despite their common history, the adjustment of both networks in the past and also nowadays, were done separately as block adjustments. Another factor contributing to this difference may be the fact that from these two countries, Slovakia is the more mountainous one. The last column *TEST* in previously mentioned table stands for the standard deviation computed from model testing. That means the use of previously reserved 10% of the GNSS/levelling points. Values were interpolated from created model and then compared with the value computed for the individual points.

Comparison of results between the use of EGM08 and EIGEN-6C4 shows the difference in δR approximately 2 cm for the territory of Slovakia. For the solution calculated only for the Czech Republic, the δR differs in range of a few millimetres.

The GGFMs solutions using XGM2019e were split into two parts. The first solution was achieved with the gravity potential computed up to degree and order 2190 and the second one up to maximum available degree and order, i.e. 5540. A similar pattern shows as in the previous case as for the territory of the Czech Republic the difference between two solutions is most likely negligible, but for the territory of the Slovak Republic, there is difference mainly in north-south tilt parameter. The main hypothesis is that in the direction from south to north the terrain elevation rises. This and higher frequencies included in the solution, i.e. using all available coefficients of the model, may actually cause this effect.

³Baltic Vertical Datum After Adjustment

Using the values of the radial offset for LVDs, the $W_{0,i}$ can be computed for both territories. In the table 2.2, the values for local $W_{0,i}$ are summarized using different models and level ellipsoids. It is clear that such value is independent of the used level ellipsoid. For the territory of the Czech Republic, the table shows that at the centimetre level precision the $W_{0,i}$ is quite independent of the model used. For more mountainous Slovak Republic this statement is not true.

Tab. 2.1: Summation of all the computations based on the different data usage [author].

Model used	Datum shift [m]		Tilt [m/100km]		$\Delta\zeta$ [m]		Error [m]		Test [m]		
	δR	STD	a	STD	b	STD	average	median	min [m]	max [m]	STD
EGM08	-0,072	$\pm 0,0004$	0,0321	$\pm 0,0010$	-0,0088	$\pm 0,0004$	-0,072	-0,073	-0,178	0,045	$\pm 0,0190$
EIGEN-6C4	-0,093	$\pm 0,0004$	0,0128	$\pm 0,0010$	-0,0021	$\pm 0,0004$	-0,093	-0,092	-0,195	0,007	$\pm 0,0190$
XGM2019e - 2190	-0,091	$\pm 0,0006$	0,0110	$\pm 0,0015$	-0,0097	$\pm 0,0006$	-0,091	-0,091	-0,236	0,054	$\pm 0,0220$
XGM2019e - 5540	-0,096	$\pm 0,0006$	0,0051	$\pm 0,0014$	-0,0101	$\pm 0,0006$	-0,096	-0,097	-0,223	0,041	$\pm 0,0210$
EGM08	-0,078	$\pm 0,0006$	-0,0098	$\pm 0,0011$	0,0019	$\pm 0,0006$	-0,078	-0,079	-0,181	0,020	$\pm 0,0130$
EIGEN-6C4	-0,081	$\pm 0,0006$	-0,0233	$\pm 0,0010$	-0,0043	$\pm 0,0006$	-0,081	-0,081	-0,195	0,023	$\pm 0,0130$
XGM2019e - 2190	-0,083	$\pm 0,0009$	-0,0244	$\pm 0,0015$	-0,0081	$\pm 0,0008$	-0,083	-0,083	-0,238	0,052	$\pm 0,0150$
XGM2019e - 5540	-0,086	$\pm 0,0009$	-0,0247	$\pm 0,0015$	-0,0089	$\pm 0,0008$	-0,086	-0,085	-0,239	0,044	$\pm 0,0140$
EGM08	-0,074	$\pm 0,0004$	0,0026	$\pm 0,0005$	0,0016	$\pm 0,0002$	-0,074	-0,075	-0,171	0,023	-
EIGEN-6C4	-0,089	$\pm 0,0004$	0,0017	$\pm 0,0005$	-0,0021	$\pm 0,0002$	-0,089	-0,089	-0,190	0,007	-
XGM2019e - 2190	-0,088	$\pm 0,0005$	-0,0064	$\pm 0,0007$	-0,0056	$\pm 0,0003$	-0,088	-0,089	-0,228	0,057	-
XGM2019e - 5540	-0,092	$\pm 0,0005$	-0,0088	$\pm 0,0007$	-0,0073	$\pm 0,0003$	-0,092	-0,093	-0,226	0,046	-
EGM08	0,193	$\pm 0,0004$	0,0320	$\pm 0,0010$	-0,0088	$\pm 0,0004$	0,193	0,192	0,087	0,310	$\pm 0,0190$
EIGEN-6C4	0,172	$\pm 0,0004$	0,0127	$\pm 0,0010$	-0,0021	$\pm 0,0004$	0,172	0,173	0,070	0,272	$\pm 0,0190$
XGM2019e - 2190	0,174	$\pm 0,0006$	0,0110	$\pm 0,0015$	-0,0097	$\pm 0,0006$	0,174	0,174	0,029	0,319	$\pm 0,0220$
XGM2019e - 5540	0,169	$\pm 0,0006$	0,0051	$\pm 0,0014$	-0,0101	$\pm 0,0006$	0,169	0,168	0,042	0,306	$\pm 0,0210$
EGM08	0,187	$\pm 0,0006$	-0,0098	$\pm 0,0011$	0,0019	$\pm 0,0006$	0,187	0,186	0,084	0,285	$\pm 0,0130$
EIGEN-6C4	0,184	$\pm 0,0006$	-0,0233	$\pm 0,0010$	-0,0043	$\pm 0,0006$	0,184	0,184	0,070	0,288	$\pm 0,0130$
XGM2019e - 2190	0,182	$\pm 0,0009$	-0,0245	$\pm 0,0015$	-0,0081	$\pm 0,0008$	0,182	0,182	0,027	0,317	$\pm 0,0150$
XGM2019e - 5540	0,179	$\pm 0,0009$	-0,0248	$\pm 0,0015$	-0,0089	$\pm 0,0008$	0,179	0,181	0,026	0,309	$\pm 0,0140$
EGM08	0,191	$\pm 0,0004$	0,0025	$\pm 0,0005$	0,0016	$\pm 0,0002$	0,191	0,190	0,094	0,288	-
EIGEN-6C4	0,176	$\pm 0,0004$	0,0017	$\pm 0,0005$	-0,0021	$\pm 0,0002$	0,176	0,176	0,075	0,272	-
XGM2019e - 2190	0,177	$\pm 0,0005$	-0,0064	$\pm 0,0007$	-0,0056	$\pm 0,0003$	0,177	0,176	0,037	0,322	-
XGM2019e - 5540	0,173	$\pm 0,0005$	-0,0088	$\pm 0,0007$	-0,0073	$\pm 0,0003$	0,173	0,172	0,039	0,311	-
Slovakia	$W_0 = 62636856,0 \text{ m}^2\text{s}^{-2}$										
Czechia	$W_0 = 62636853,4 \text{ m}^2\text{s}^{-2}$										
Combined	$W_0 = 62636856,0 \text{ m}^2\text{s}^{-2}$										

Tab. 2.2: The value of $W_{0,i}$ for LVDs used on territories of the Czech Republic and the Slovak Republic using different GGFMs [author].

Territory	W_0	Used model	Datum shift [m]		$W_{0,i}$ [m^2s^{-2}]	$\delta W_{0,i}$ [m^2s^{-2}]
			δR	STD		
Slovakia	$W_0 = 62636856.0$ [m^2s^{-2}]	EGM08	-0.072	0.0004	62636855.29	0.71
		EIGEN-6C4	-0.093	0.0004	62636855.09	0.91
		XGM2019e up to 2190	-0.091	0.0006	62636855.11	0.89
		XGM2019e up to 5540	-0.096	0.0006	62636855.06	0.94
Czechia		EGM08	-0.078	0.0006	62636855.23	0.77
		EIGEN-6C4	-0.081	0.0006	62636855.20	0.80
		XGM2019e up to 2190	-0.083	0.0009	62636855.18	0.82
		XGM2019e up to 5540	-0.086	0.0009	62636855.16	0.84
Combined		EGM08	-0.074	0.0004	62636855.27	0.73
		EIGEN-6C4	-0.089	0.0004	62636855.12	0.88
		XGM2019e up to 2190	-0.088	0.0005	62636855.13	0.87
		XGM2019 up to 5540	-0.092	0.0005	62636855.09	0.91
Slovakia	$W_0 = 62636853.4$ [m^2s^{-2}]	EGM08	0.193	0.0004	62636855.30	-1.90
		EIGEN-6C4	0.172	0.0004	62636855.10	-1.70
		XGM2019e up to 2190	0.174	0.0006	62636855.12	-1.72
		XGM2019e up to 5540	0.169	0.0006	62636855.07	-1.67
Czechia		EGM08	0.187	0.0006	62636855.24	-1.84
		EIGEN-6C4	0.184	0.0006	62636855.21	-1.81
		XGM2019e up to 2190	0.182	0.0009	62636855.19	-1.79
		XGM2019e up to 5540	0.179	0.0009	62636855.16	-1.76
Combined		EGM08	0.191	0.0004	62636855.28	-1.88
		EIGEN-6C4	0.176	0.0004	62636855.13	-1.73
		XGM2019e up to 2190	0.177	0.0005	62636855.14	-1.74
		XGM2019e up to 5540	0.173	0.0005	62636855.10	-1.70

2.3.1 Models - FAST GBVP

All the models computed for the purpose of this doctoral thesis are included on the DVD to the doctoral thesis. The *NODATA* area for these models is basically outside the countries borders. These values are by default set to -9999.999 , the rest of the data is stored in millimetre precision. The resolution in the latitude and also in the longitude direction is $7.2''$.

On figure 2.1 the connection corrections for joining the LVD of the Slovak Republic with the GVRS represented by GGFm EGM08 and $W_0 = 62\,636\,856.0\text{m}^2\text{s}^{-2}$ is shown. Also the histograms (figure 2.2) describing the distribution of δR and v_i are introduced. The histograms are organized in pairs where each left histogram (a) shows the distribution of the radial distortion term and histogram on the right sight (b) shows the error distribution when the final model was tested using the spare 10% of the points. It is clear, that all histograms have normal distribution.

For the territory of the Czech Republic the connection corrections are displayed on figure 2.3 and related histograms are in figure 2.4.

The histograms are organized in pairs where each left histogram (a) shows the distribution of the radial distortion term and histogram on the right sight (b) shows the error distribution when the final model was tested using the spare 10% of the points. It is clear, that all histograms have normal distribution.

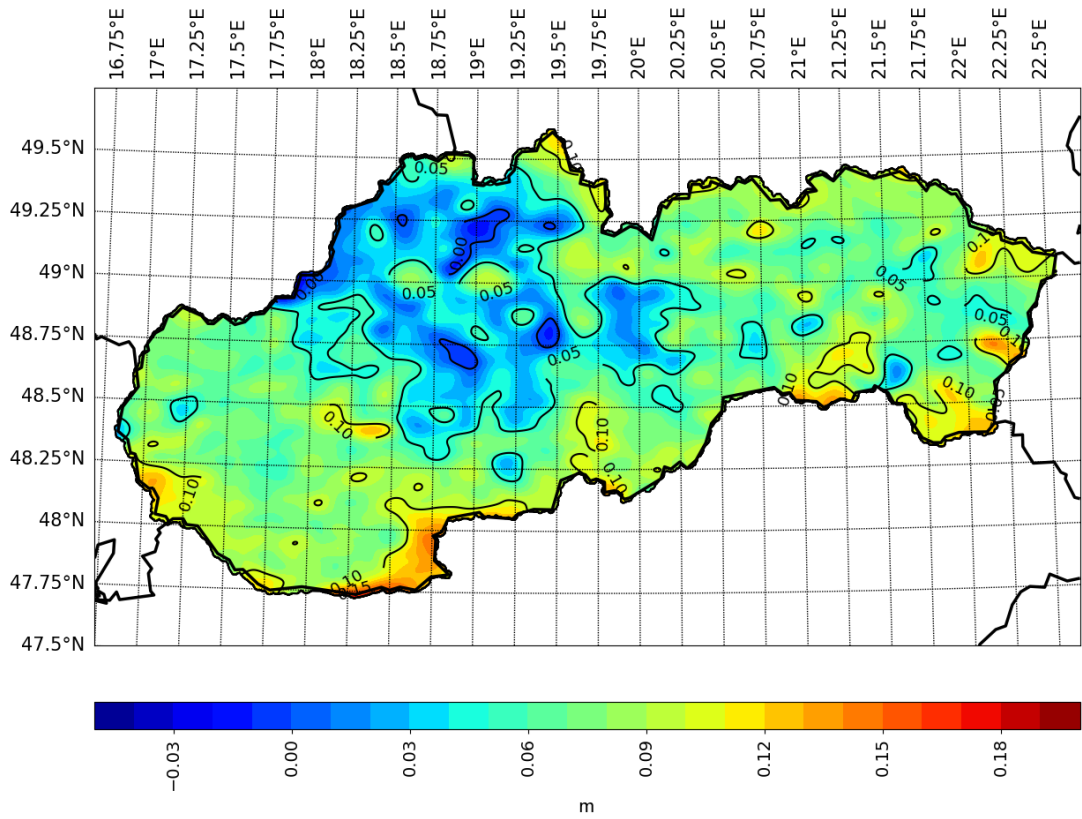


Fig. 2.1: The differences between the KHD and the WHS represented by GGFM EGM08, $W_0 = 62\,636\,856.0\text{ m}^2\text{ s}^{-2}$, $GM = 3.986004415 \cdot 10^{14}\text{ m}^3\text{ s}^{-2}$ for the territory of the Slovak Republic. Average value from the raster layer $\delta R = 0.067 \pm 0.027\text{ m}$, data range $[-0.026, 0.172]\text{ m}$ [author].

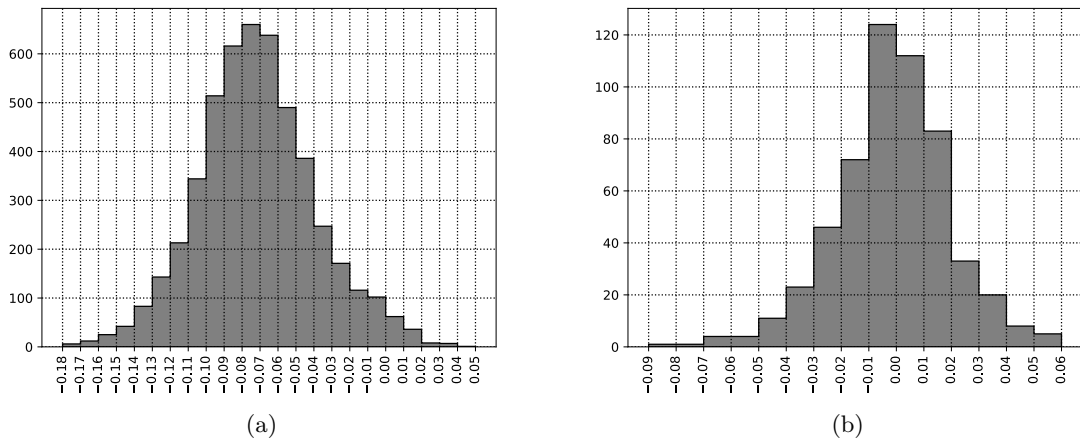


Fig. 2.2: Histograms for the connection between the KHD and the WHS for the territory of the Slovak Republic. WHS is represented by GGFM EGM08, $W_0 = 62\,636\,856.0\text{ m}^2\text{ s}^{-2}$, $GM = 3.986004415 \cdot 10^{14}\text{ m}^3\text{ s}^{-2}$. The figure (a) shows the errors distribution for the data used for model creation, the figure (b) shows errors distribution when tested [author].

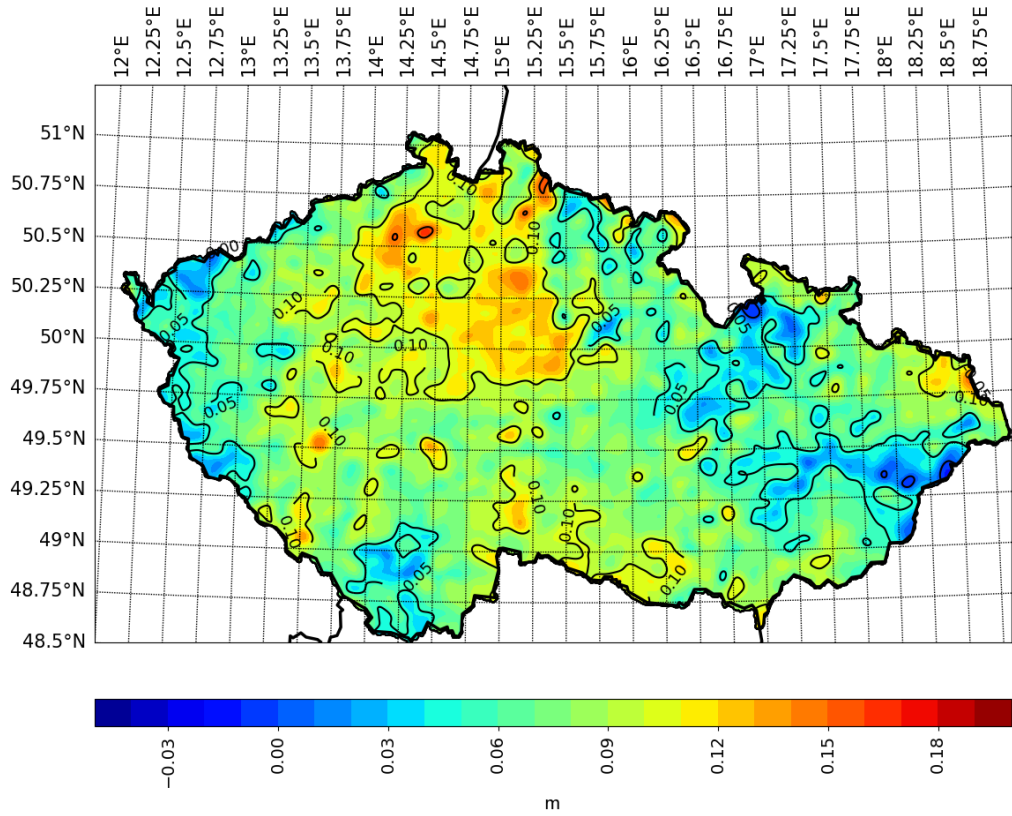


Fig. 2.3: The differences between the KHD and the WHS represented by GGFM EGM08, $W_0 = 62\,636\,856.0\text{ m}^2\text{ s}^{-2}$, $GM = 3.986004415 \cdot 10^{14}\text{ m}^3\text{ s}^{-2}$ for the territory of the Czech Republic. Average value from the raster layer $\delta R = 0.077 \pm 0.025\text{ m}$, data range $[-0.013, 0.166]\text{ m}$ [author].

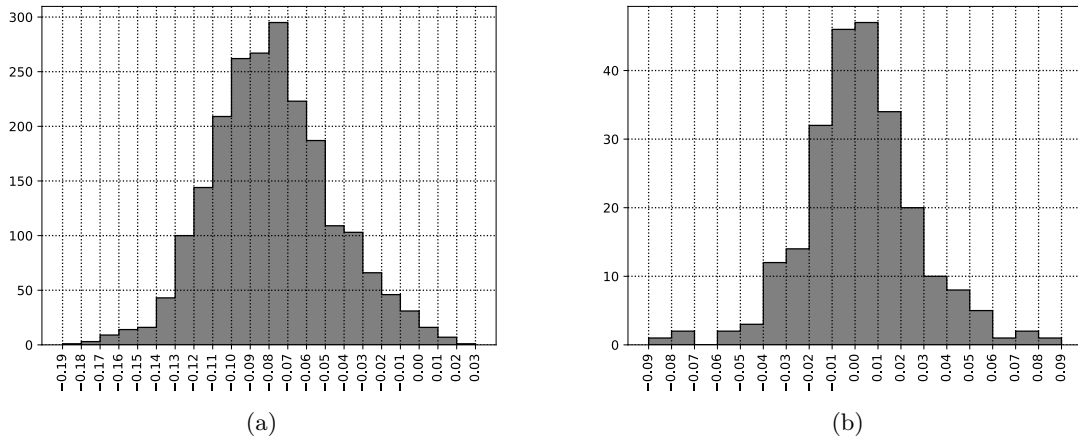


Fig. 2.4: Histograms for the connection between the KHD and WHS for the territory of the Czech Republic. WHS is represented by GGFM EGM08, $W_0 = 62\,636\,856.0\text{ m}^2\text{ s}^{-2}$, $GM = 3.986004415 \cdot 10^{14}\text{ m}^3\text{ s}^{-2}$. The figure (a) shows the errors distribution for the data used for model creation, the figure (b) shows errors distribution when tested [author].

2.4 Classical GBVP approach

In this section, the results of the second method used in this doctoral thesis are summarized. Similarly to the previous section, the results are split into table section, the model's figure section and the histogram section. It is important to mention how the models were created. Using the slightly modified RCR (see section 1.11) method the disturbing potential was obtained. The computation of GGFM used ellipsoid WGS84 as reference ellipsoid and so the normal gravity field is then related to its constants. All the computations were done in the zero-tide system and only the results were transformed into the mean-tide system in order to compute the connection. So to use the commonly accepted W_0 , the equation 2.5 has to be used

$$\Delta W_0 = W_0 - U_0, \quad (2.5)$$

where U_0 is related to ellipsoid WGS84.

For example, $\Delta W_0 = 62\,636\,856.0 - 62\,636\,851.714 = 4.286 \text{ m}^2\text{s}^{-2}$ may seem to be some kind of error but when computing the height anomalies directly from the models such as EGM08 or EIGEN-6C4, the zero degree term is missing. This term converts geoid undulations that are intrinsically referenced to an ideal mean-earth ellipsoid into undulations that are referenced to WGS84. The value of -41 cm derives from a mean-earth ellipsoid for which the estimated parameters in the tide free system are: $a = 6\,378\,136.58 \text{ m}$ and $f^{-1} = 298.257686$ ([100]). The difference ΔW_0 must be taken into account. For the case of using different values of geocentric gravity constant, the second term is ΔGM . Consider the case when the GM value is different for level ellipsoid and the used GGFM:

$$\Delta GM = GM^{GGFM} - GM^{ELL}, \quad (2.6)$$

where GM^{GGFM} is the value used by GGFM and GM^{ELL} is referred to the reference ellipsoid. To transform the term ΔGM to potential units, it is necessary to divide the term by radius of the reference sphere $\Delta GM/R$. This step is particularly important for example when the millimetre precision is required, taking into account the GM value from reference ellipsoid WGS84 and GGFM EGM08. In this case, the difference transformed to geopotential units is $-0.047 \text{ m}^2\text{s}^{-2}$.

For a practical demonstration, all the calculations were done in the zero-tide system. And in the end, it was transformed into the mean-tide system. Solving the fixed-GBVP (equations 1.23 and 1.26) and including the members in equations 2.5 and 2.6 provides the value which represents the GVRs:

$$T^{GVRs} = \frac{\Delta GM}{R} - \frac{\Delta W_0}{\gamma} + T + T_0 + T_1 \quad . \quad (2.7)$$

Where the T stands for the contribution of low degree harmonics (from 0 to 164), T_0 is the contribution of the zero term of Molodensky's series and the T_1 is the contribution of the first member of the expansion (equations 1.20 and 1.27). The T term contains around 98% of the signal, T_0 contributes at the level of decimetres and T_1 at the centimetre level, since T_i are geopotential numbers they have to be converted to height anomalies (eq. 1.27).

Since for these computations the slightly modified Remove-Compute-Restore method was used, the higher terms than T_1 were neglected. Even for the mountainous areas of High Tatras for the integration radius ($\approx 122 \text{ km}$), the higher terms can be omitted and we will still be able to reach the cm precision. For the practical computations the equation 1.50 was used. Also all the computations were done using the developed package PhysGeo.

Since the LVDs for the territory of the Czech Republic and the Slovak Republic use the mean tide system, the T^{GVRs} was converted to $\zeta^{GVRs,ZT}$ and then transformed into the mean-tide system.

2.5 RTM contribution

In this doctoral thesis, the RTM method was used to model the missing frequencies in used GGFMs. Then the results were applied to solution obtained from gravity data computed from the EGM08 and EIGEN-6C4. The RTM technique was performed while using the DEM GMTED10 and the MES model DTM2006.0⁴. For different GGFMs it can be required to use different model for MES. However, the EIGEN-6C4 has been generated by using data from LAGEOS, GRACE RL03 GRGS, GOCE-SGG (November 2009 till October 2013) plus a $2' \times 2'$ free-air gravity anomaly grid (altimetry over the

⁴Full name *Coeff_Height_and_Depth_to2190_DTM2006*

oceans, EGM08 over the continents). Since the high frequencies in EIGEN-6C4 over the continents are derived from EGM08, the same reference surface was used for both models. The constant density value of $2670 \text{ kg} \cdot \text{m}^{-3}$ for land areas was used. However, some test calculations onshore used $1030 \text{ kg} \cdot \text{m}^{-3}$ for sea area.

Tab. 2.3: The brief description of the RTM contribution [author].

	RTM with 10 km radius		RTM with 18 km radius	
Territory	(a) Czechia	(b) Slovakia	(a) Czechia	(b) Slovakia
Data range [m]	[-0.05, +0.03]	[-0.06, +0.03]	[-0.06, +0.02]	[-0.07, +0.03]
Average value [m]	0.004	0.004	0.001	0.001
STD of avg. value [m]	0.006	0.007	0.006	0.007

2.5.1 Models - classic GBVP

To continue in the previously used notations, let us consider the ζ^{LVD} for LVD and ζ^{GVRs} for GVRs. The difference is then calculated as:

$$\Delta\zeta = \zeta^{GVRs} - \zeta^{LVD} \rightarrow \zeta^{GVRs} = \Delta\zeta + \zeta^{LVD}. \quad (2.8)$$

Using equation 2.1 for such defined values $\Delta\zeta$ leads to summary in the table 2.4. Results are divided for both used values of W_0 and also for the territory of the Czech Republic and the Slovak Republic. The columns labelled as *error* stand for the residual value, the minimum and maximum values are listed. It is important also to clarify what quasi-geoid models were used. For the territory of the Czech Republic the quasi-geoid model used is *Podrobný kvazigeoid QGZÚ-2013*⁵ ([101]) and for the Slovak Republic *DVRM05* ([102]).

The solution of GBVP was combined with the RTM technique. The computation radius used for the RTM was set to either 10 km or 18 km. As it was explained in section 1.10.1 Harmonic correction, the harmonic correction was not applied, since the GGfMs which are expressed as a series of spherical harmonics are not capable of handling the non-harmonic functions. That means that the values obtained from GGfM above the reference ellipsoid act as harmonic functions. That applies also for points which are in reality inside the masses. The non-harmonicity of functions inside the masses is not part of GGfM and should not be corrected.

In the table the results are listed for these GGfMs: EGM08, EGM08 + RTM-10 km and EGM08 + RTM-18 km. The same process was done with the GGfM EIGEN-6C4. When examining the results it is clear that the used radius significantly impacts the values δR and a but the tilt in east-west direction - b , does not display any significant change at all. Therefore, the cut-off distance for RTM plays a significant and important role. For the less mountainous territory of the Czech Republic, the tilt value a in north-south direction is not changing significantly. This brings up the hypothesis that for mountainous areas, the RTM technique should be put to test and 'redeveloped'. For the GfM, the average density value $2670 \text{ kg} \cdot \text{m}^{-3}$ was used. In report [103], the average density values for Tatras' types of sediments and rocks is in interval $2600 - 2800 \text{ kg} \cdot \text{m}^{-3}$. Also, in the south-center part of Slovak Republic, there are some density anomalies, where the density of rocks and sediments are in range $2000 - 2670 \text{ kg} \cdot \text{m}^{-3}$. The density differences alone can theoretically contribute in relative scale up to 25% for quantity computed by GfM.

Solving the GBVP was combined with the RTM technique. The computation radius used for the RTM was set to either 10 km or 18 km. As it was explained in section 1.10.1 Harmonic correction, the harmonic correction was not applied, since the GGfMs which are expressed as a series of spherical harmonics are not capable of handling the non-harmonic functions. That means that the values obtained from GGfM above the reference ellipsoid act as harmonic functions. That applies also for points which are in reality inside the masses. The non-harmonicity of functions inside the masses is not part of GGfM and should not be corrected. Also the HC in the listed form is for gravity anomalies.

In the table the results are listed for these GGfMs: EGM08, EGM08 + RTM-10 km and EGM08 + RTM-18 km. The same process was done with the GGfM EIGEN-6C4. When examining the results it is clear that the used radius significantly impacts the values δR and a but the tilt in east-west

⁵translation: Detailed quasi-geoid QGZÚ-2013.

Tab. 2.4: Summation of all the computations based on the different data usage [author].

Model used	Datum shift [m]		Tilt [m/100km]			$\Delta\zeta$ [m]			error [m]	
	δR	STD	a	STD	b	STD	average	median	min [m]	max [m]
Slovakia $W_0=62636856.0 \text{ m}^2\text{s}^{-2}$	EGM08	$\pm 0,0004$	0,042	$\pm 0,0010$	-0,018	$\pm 0,0007$	0,363	0,363	-0,090	0,090
	EGM08+r10 km	$\pm 0,0004$	0,044	$\pm 0,0010$	-0,018	$\pm 0,0007$	0,369	0,368	-0,089	0,090
	EGM08+r18 km	$\pm 0,0004$	0,042	$\pm 0,0010$	-0,018	$\pm 0,0007$	0,363	0,363	-0,090	0,090
	EIGEN-6C4	$\pm 0,0004$	0,023	$\pm 0,0010$	-0,003	$\pm 0,0007$	0,344	0,345	-0,089	0,090
	EIGEN-6C4+r10 km	$\pm 0,0004$	0,026	$\pm 0,0010$	-0,004	$\pm 0,0007$	0,350	0,351	-0,092	0,092
	EIGEN-6C4+r18 km	$\pm 0,0004$	0,024	$\pm 0,0010$	-0,004	$\pm 0,0007$	0,344	0,345	-0,093	0,093
	XGM2019e_upto2190	$\pm 0,0006$	0,017	$\pm 0,0014$	-0,014	$\pm 0,0009$	0,306	0,307	-0,129	0,128
	XGM2019e_upto5140	$\pm 0,0006$	0,009	$\pm 0,0014$	-0,013	$\pm 0,0009$	0,303	0,303	-0,123	0,122
	EGM08	$\pm 0,0007$	0,009	$\pm 0,0011$	0,003	$\pm 0,0009$	0,372	0,369	-0,093	0,095
	EGM08+r10 km	$\pm 0,0007$	0,009	$\pm 0,0011$	0,003	$\pm 0,0009$	0,377	0,374	-0,095	0,097
Czechia	EGM08+r18 km	$\pm 0,0007$	0,009	$\pm 0,0011$	0,003	$\pm 0,0009$	0,372	0,369	-0,093	0,095
	EIGEN-6C4	$\pm 0,0006$	-0,011	$\pm 0,0010$	-0,007	$\pm 0,0008$	0,369	0,368	-0,088	0,088
	EIGEN-6C4+r10 km	$\pm 0,0006$	-0,010	$\pm 0,0011$	-0,006	$\pm 0,0009$	0,373	0,373	-0,092	0,092
	EIGEN-6C4+r18 km	$\pm 0,0006$	-0,011	$\pm 0,0011$	-0,006	$\pm 0,0009$	0,368	0,368	-0,092	0,090
	XGM2019e_upto2190	$\pm 0,0009$	-0,015	$\pm 0,0014$	-0,012	$\pm 0,0012$	0,325	0,325	-0,126	0,126
	XGM2019e_upto5140	$\pm 0,0009$	-0,017	$\pm 0,0015$	-0,012	$\pm 0,0012$	0,323	0,324	-0,126	0,127
	EGM08	$\pm 0,0004$	0,042	$\pm 0,0010$	-0,018	$\pm 0,0007$	0,098	0,098	-0,090	0,090
	EGM08+r10 km	$\pm 0,0004$	0,044	$\pm 0,0010$	-0,018	$\pm 0,0007$	0,104	0,103	-0,089	0,090
	EGM08+r18 km	$\pm 0,0004$	0,042	$\pm 0,0010$	-0,018	$\pm 0,0007$	0,098	0,098	-0,090	0,090
	EIGEN-6C4	$\pm 0,0004$	0,023	$\pm 0,0010$	-0,003	$\pm 0,0007$	0,079	0,080	-0,089	0,090
Slovakia $W_0=62636853.4 \text{ m}^2\text{s}^{-2}$	EIGEN-6C4+r10 km	$\pm 0,0004$	0,026	$\pm 0,0010$	-0,004	$\pm 0,0007$	0,085	0,086	-0,092	0,092
	EIGEN-6C4+r18 km	$\pm 0,0004$	0,024	$\pm 0,0010$	-0,004	$\pm 0,0007$	0,079	0,080	-0,093	0,093
	XGM2019e_upto2190	$\pm 0,0006$	0,017	$\pm 0,0014$	-0,014	$\pm 0,0009$	0,041	0,042	-0,129	0,128
	XGM2019e_upto5140	$\pm 0,0006$	0,009	$\pm 0,0014$	-0,013	$\pm 0,0009$	0,038	0,038	-0,123	0,122
	EGM08	$\pm 0,0007$	0,009	$\pm 0,0011$	0,003	$\pm 0,0009$	0,107	0,103	-0,093	0,095
	EGM08+r10 km	$\pm 0,0007$	0,009	$\pm 0,0011$	0,003	$\pm 0,0009$	0,112	0,108	-0,095	0,097
	EGM08+r18 km	$\pm 0,0007$	0,009	$\pm 0,0011$	0,003	$\pm 0,0009$	0,107	0,103	-0,093	0,095
	EIGEN-6C4	$\pm 0,0006$	-0,011	$\pm 0,0010$	-0,007	$\pm 0,0008$	0,104	0,103	-0,088	0,088
	EIGEN-6C4+r10 km	$\pm 0,0006$	-0,010	$\pm 0,0011$	-0,006	$\pm 0,0009$	0,108	0,108	-0,092	0,092
	EIGEN-6C4+r18 km	$\pm 0,0006$	-0,010	$\pm 0,0011$	-0,006	$\pm 0,0009$	0,103	0,103	-0,092	0,090
Czechia $W_0=62636853.4 \text{ m}^2\text{s}^{-2}$	XGM2019e_upto2190	$\pm 0,0009$	-0,015	$\pm 0,0014$	-0,012	$\pm 0,0012$	0,059	0,060	-0,126	0,126
	XGM2019e_upto5140	$\pm 0,0009$	-0,017	$\pm 0,0015$	-0,012	$\pm 0,0012$	0,058	0,059	-0,126	0,127

direction - b , does not display any significant change at all, therefore, the cut-off distance for RTM plays a significant and important role. For the less mountainous territory of the Czech Republic, the tilt value a in north-south direction is not changing significantly. This brings up the hypothesis that for mountainous areas, the RTM technique should be put to test and 'redeveloped'. Some form of terrain simplification (low-pass filter, area averaging algorithm, etc.) should be considered. Also for the FGM, the average density value $2670 \text{ kg} \cdot \text{m}^{-3}$ was used. In report [103], the average density

values for Tatras' types of sediments and rocks is in interval $2\,600 - 2\,800 \text{ kg} \cdot \text{m}^{-3}$. Also, in the South-Center part of Slovak Republic, there are some density anomalies, where the density of rocks and sediments is in range $2\,000 - 2\,670 \text{ kg} \cdot \text{m}^{-3}$. The density differences alone can theoretically contribute in relative scale up to 25% for quantity computed by FGM.

The connection corrections $\Delta\zeta$ are shown on following figures. For the figures 2.5 and 2.6 the $W_0 = 62\,636\,856.0 \text{ m}^2\text{s}^{-2}$. The first figure shows the use of only GGM EGM08⁶ alone, second figure shows the RTM with the integration radius 18 km. The presence of the higher-frequencies obtained by RTM technique is clearly visible. The unexpected negative $\Delta\zeta$ are shown for the area of the capital city of the Czech Republic - Prague and the mountain chain Little Carpathians, located in the Western part of Slovakia.

The connection corrections $\Delta\zeta$ while using the $W_0 = 62\,636\,853.4 \text{ m}^2\text{s}^{-2}$ is basically the same with just constant 'height shift'.

When returning to the equation 2.1, there are two important terms. The first one is the connection correction $\Delta\zeta$ and the second one is the term for residual value v . The residual value is obtained from least square adjustment process. For the figure 2.5 the related histograms are figures 2.7 and 2.8, respectively. For the figure 2.6 the related histograms are figures 2.9 and 2.10. The histograms are organized in pairs where each left histogram (a) shows the distribution for the connection correction $\Delta\zeta$, histogram (b) shows the residuals from the least square adjustment.

When examining closely the histograms on the left side, it reveals some systematic error is involved in the process of computing the connection correction, especially for the territory of the Slovak Republic. Let's for example take the histogram (a) on figure 2.8. All of these $\Delta\zeta$ values are located in East Slovakia and correspond with the azure/blue areas displayed on figure 2.5. This effect may be caused by some systematic error in original GNSS/levelling data, residual anomalies in GGMs, etc.

⁶The models which are not shown in this chapter can be found in the enclosed DVD of the doctoral thesis.

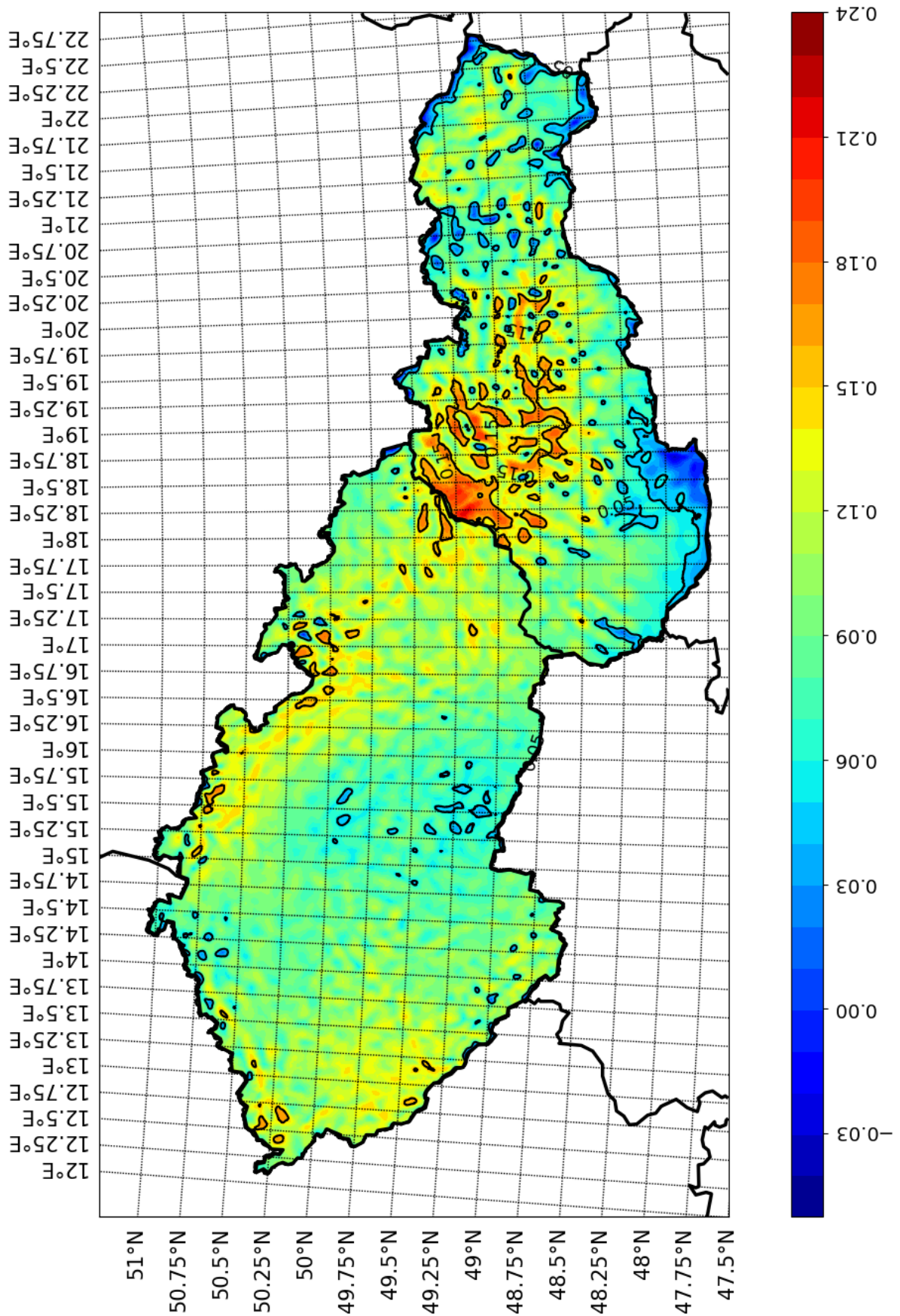


Fig. 2.5: Connection between the KHD and WHS. WHS is represented by GGFM EGM08 and by $W_0 = 62\,636\,856.0\text{m}^2\text{s}^{-2}$ [author].

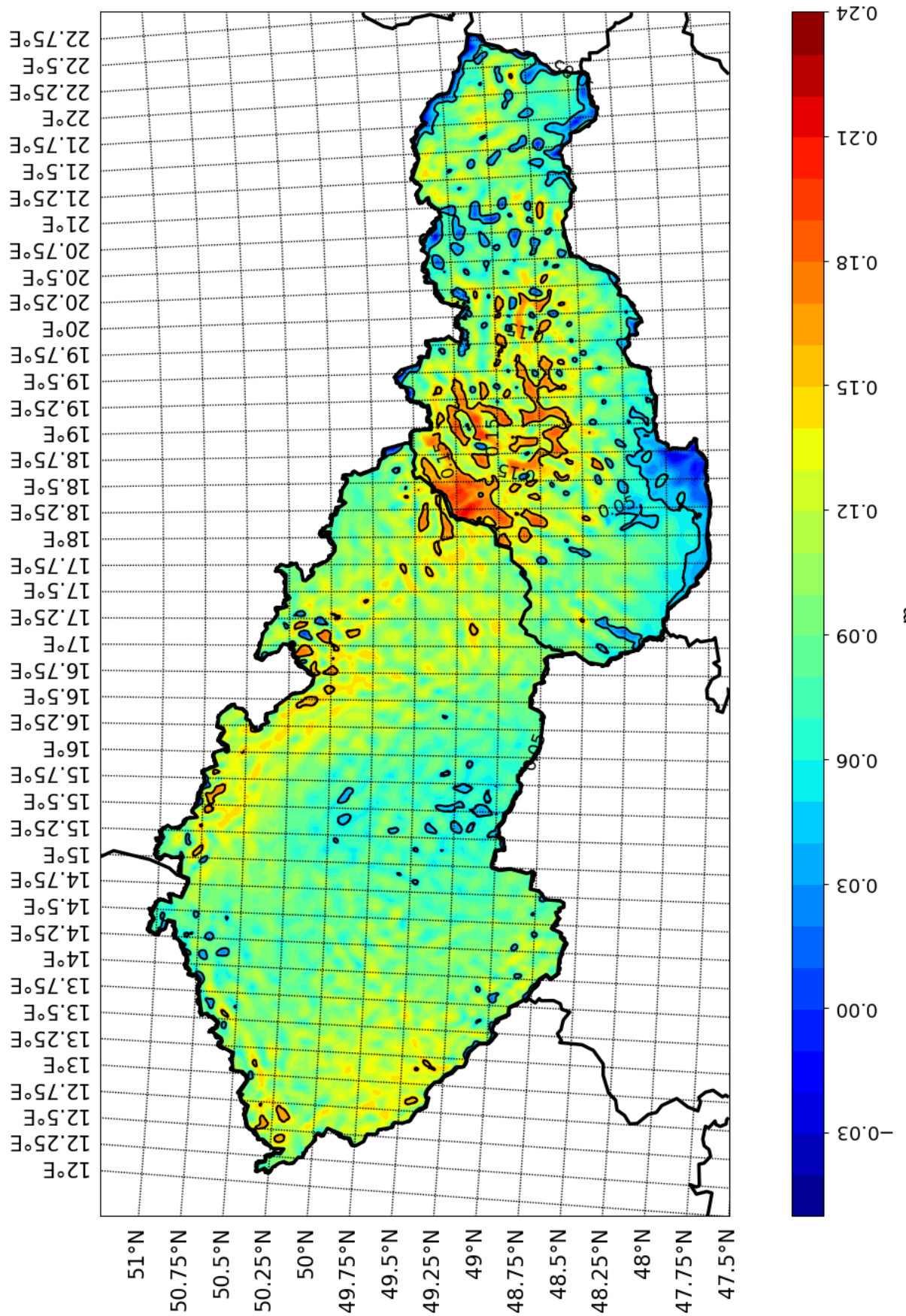


Fig. 2.6: Connection between the KHD and WHS. WHS is represented by GGFM EGM08 combined with residual terrain modelling (radius = 18 km) and by $W_0 = 62\,636\,856.0\text{m}^2\text{s}^{-2}$ [author].

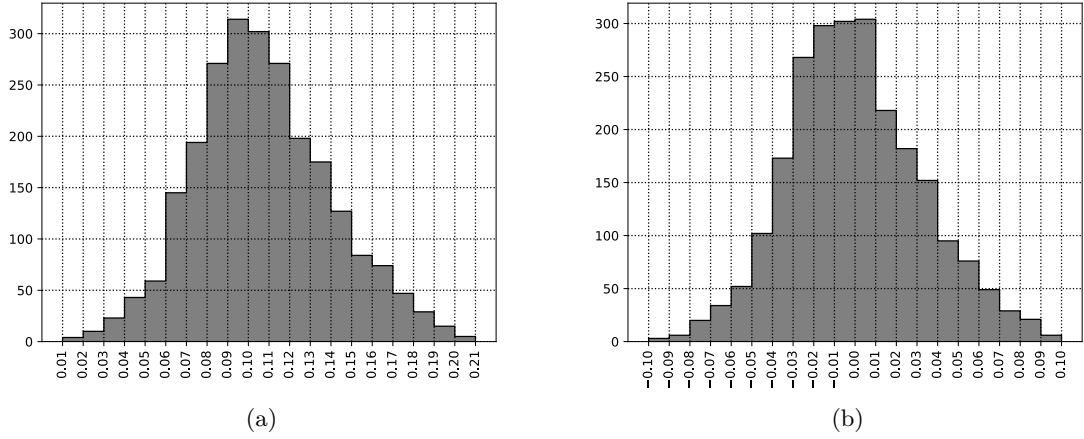


Fig. 2.7: Histograms for the connection between the KHD and WHS for the territory of the Czech Republic using the classical GBVP approach. WHS represented by GGFM EGM08, $W_0 = 62\,636\,856.0\text{ m}^2\text{ s}^{-2}$. The figure (a) shows the $\Delta\zeta$ distribution. Figure (b) shows residual distribution [author].

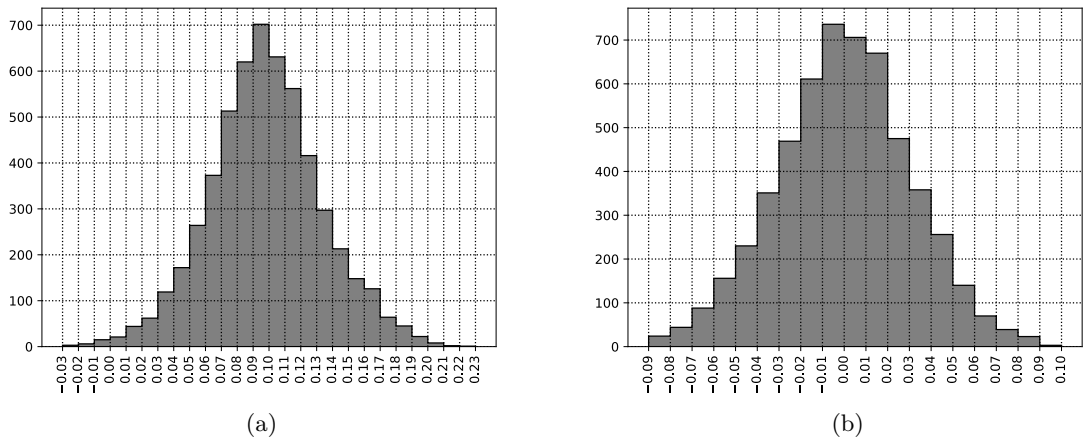


Fig. 2.8: Histograms for the connection between the KHD and WHS for the territory of the Slovak Republic using the classical GBVP approach. WHS represented by GGFM EGM08, $W_0 = 62\,636\,856.0\text{ m}^2\text{ s}^{-2}$. The figure a) shows the $\Delta\zeta$ distribution. Figure (b) shows residual distribution [author].

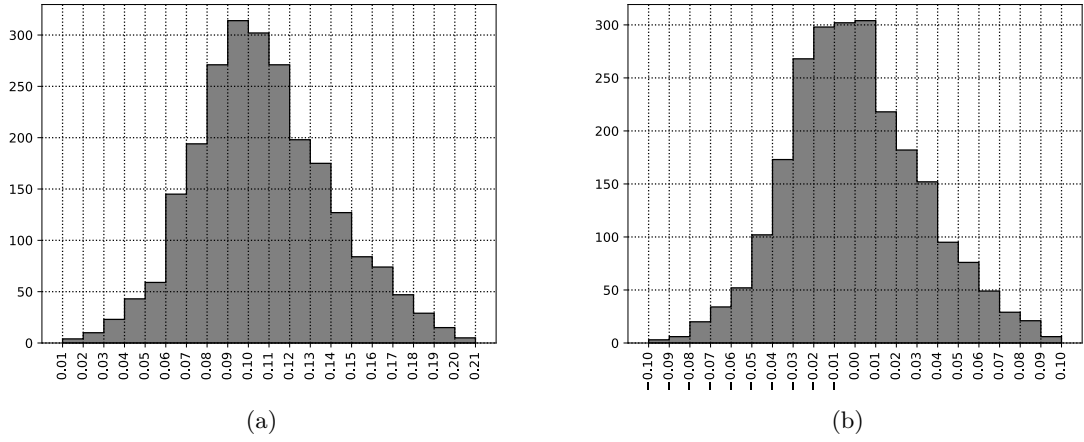


Fig. 2.9: Histograms for the connection between the KHD and WHS for the territory of the Czech Republic using the classical GBVP approach. WHS represented by GGFM EGM08 with residual terrain modelling (radius = 18 km), $W_0 = 62\,636\,856.0\text{ m}^2\text{ s}^{-2}$. The figure a) shows the $\Delta\zeta$ distribution. Figure (b) shows residual distribution [author].

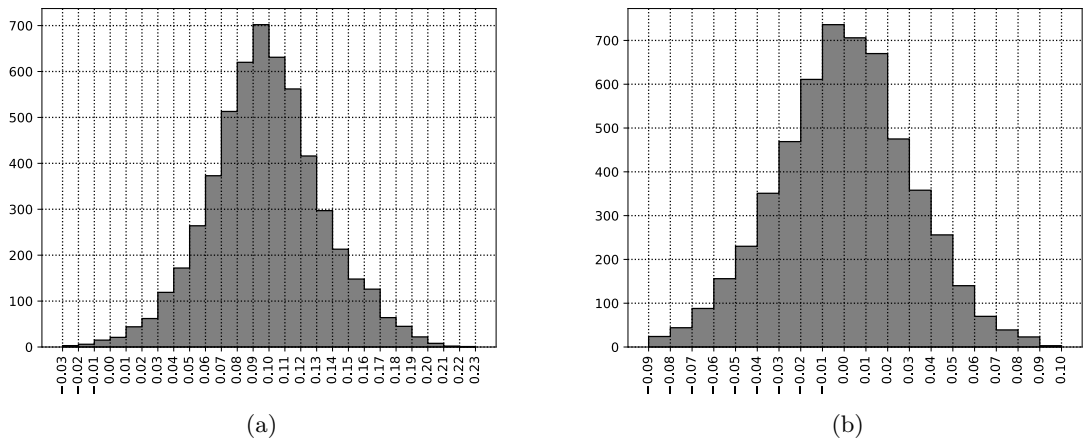


Fig. 2.10: Histograms for the connection between the KHD and WHS for the territory of the Slovak Republic using the classical GBVP approach. WHS represented by GGFM EGM08 with residual terrain modelling (radius = 18 km), $W_0 = 62\,636\,856.0\text{ m}^2\text{ s}^{-2}$. The figure a) shows the $\Delta\zeta$ distribution. Figure (b) shows residual distribution [author].

3 CONCLUSIONS AND OUTLOOK

The main goal of this doctoral thesis was fulfilled. The purpose was to provide methods for connection between Local Vertical Datums, used on the territories of the Czech Republic and the Slovak Republic, and Global Vertical Reference Frame. In contrast to geometrically defined global terrestrial reference systems, physical height systems suffer from discrepancies up to $\pm 1 - 2$ m due to the individual definition of their local vertical datum. In order to realize a comparison of physical heights, a height system unification is required.

Following methods were suggested and introduced:

The first method tested in this doctoral thesis is distinguished as FAST GBVP. This method was derived originally from the method used for testing GGFMs.

The second method relied on solving the Molodensky's fixed GBVP (discussed in section 1.5.2 Molodensky's problem - free boundary value problem), using the gravity disturbances (δg) in numerical computations. The δg values were either computed from GGM up to maximum possible degree and order or the missing signal of the gravity field was modelled using the residual terrain modelling.

The spatial resolution of models used in this thesis differs. For models such as EIGEN-6C4 and EGM08, the resolution is around 10 km. The last model used in this doctoral thesis was XGM2019e which contains the coefficients up to degree and order 5540. This means that the spatial resolution is approximately 4 km.

The first two models were also combined with RTM where δg was computed from integration radius of 10 km and 18 km. Results showed that the cut-off distance does not have a significant impact on the computation outcome, however, the main impact of the cut-off distance is on the value of the total datum shift. Analysis of the results has also shown that for the precision at the centimetre level, the cut-off distance is practically negligible.

Close examination of the table 2.3 provides us with the fact that the change in the integration radius does not impact the average value for the datum shift. Especially when examining the results in table 2.4, it can be seen that the datum shift value δR is not influenced significantly. The values of the tilt for the LVDs of the Czech Republic and the Slovak Republic are also practically unchanged when taking the RTM effect into consideration.

When examining the results in the table 2.4, it is clearly visible that the RTM contribution to overall vertical datum shift is around 1 cm. Also the impact on the datum tilt is insignificant. The change of the integration radius slightly impacts the interval in which the RTM effect contributes to height anomalies and the impact on the vertical datum shift is imperceptible.

Analysis of computation outcomes, when using the XGM2019e model with two different degree and order levels - 2190 and 5540 respectively, has shown that the difference in the results is negligible at the cm level of precision.

The method used for geopotential models testing is fast and comfortable to use, the only data needed are the geopotential models and GNSS/levelling points. This can also become a disadvantage because of their distribution and also the quality. Most of the levelling lines are through the valleys, and for this reason, the coverage in mountainous areas is sparse or none. When the 'FAST' GBVP method was applied on the territories of the Czech Republic and the Slovak Republic, the 10 % of total number of points were not used for computing the connection correction but were used later to test this connection.

3.1 Summary of results

In this thesis, two methods were used to address the set up goal to manage the connection between the LVD and GVRs.

The first method distinguished as 'FAST GBVP' holds advantage over the second method. It is caused by the fact that it is easy to perform, and there is practically no need to obtain the gravity data from vast overlapping around the interest areas to perform numerical integration of the Stokes' or Hotine's integral. However, the gravity data are required for processing the precise levelling data. It is highly recommended to obtain sufficient data from neighbouring countries to examine the discrepancies at the borders. Also if taken into extreme case, use of this method does not require the connection of the relative and precise levelling network to tide gauge. And since the combination of the precise levelling network and GNSS measurements the connection can be computed safely at cm level precision.

The second method heavily depends on availability and quality of the gravity data for not only the territory of interest but also vast areas around that territory. For example if the remove-compute-restore technique is used, consider an integration radius of 167 km. Since in this thesis the computation of the quasi-geoid was performed that means that not only data 167 km beyond the borders are needed but also the data beyond another 167 km are needed since they are required to compute the additional member from Molodensky's series expansion. This can be a problem mainly for two reasons. The first reason is that some countries does not provide such data for public users or those data are classified, especially high frequency data that have means of an economic interest. The second problem is homogeneity of such data, since on national level the way how the gravity data are obtained may differ.

The unification of the national height reference frames based on GNSS/levelling data is an interesting and also very suitable approach to achieve the goal. Further improvements can be expected using newly adjusted National Vertical reference frames, GNSS/levelling data with higher density and also use of the results of new satellite gravity missions. Also in the future it is important to address the inconsistencies in the international standards and conventions for geometric and also gravity reference frames.

Delivered results:

- provided the theoretical background for highly precise physical reference frame
- satisfy the condition $h_{el} - h_n - \zeta = 0$ at the centimetre level
- support the determination and combination of geometric and physical heights
- establish the realisation of the GVRF and the connection between the LVDs of the Czech Republic and the Slovak Republic and such created GVRS.
- the suggestion how to treat the singularities when the closed form of the integration kernels is used

3.2 Recommendations for future work

Nowadays, the completion and new gravity measurements for the territory of the Czech Republic takes place. If the output of this measurement renewal is publicly accessible, new options for computing the connection between LVD and GVRS will open.

In this thesis, two experiments related to cut-off distance were done. One of them was using the cut-off distance 10' (suggested in [97]) which can be translated as approximately 18 km. The second experiment was using only half of the previous value (5' \approx 10 km). As it was shown in table 2.4, it does not effect the results at the centimetre level significantly. Most of the difference takes place at the millimetre level, therefore the change in the integration radius is practically negligible in this study.

For future work, the fixed-GBVP seems to be the most effective due to the availability of global data such as GGFMs (EIGEN-6C4, EGM08, etc.), DEMs (SRTM, GMTED10, ETOPO1 etc.) and local data such as GNSS/levelling points or gravity measurements.

The impact of approximation errors on the presented spherical solution in fixed-GBPV should be investigated and taken into account by suitable reductions, especially for the global geometry.

Another issue is the usage of the latest up to date DEM with the appropriately high resolution. In this study, the GMTED10 which provides sufficient coverage for Europe was used. For more precise modelling, model with higher resolution should be used. For example the latest DEM for the territory of the Czech republic is the DMR 5G¹ and has declared precision $\sigma \pm 0.18$ m for the territory without dense vegetation and $\sigma \pm 0.30$ m otherwise. The similar project is currently being in progress in Slovakia. The other option is to use other models such as SRTM3 which offers global coverage except the polar areas or the its derived products.

In the future the treatment of time-dependent components of various parameters, proper evaluation of the reference period and the period of the measurement will be required in order to achieve precision at the millimetre level. Time dependent parameters are for example $C_{2,0}$, h_n (separation of the vertical crust movements), $W_{0,i}$ for reference tide gauges, etc.

¹Translated from the Czech language: Digital elevation model of the fifth generation, originally in the Czech language: Digitální model reliéfu České republiky 5. generace. But unfortunately for scientific use provided in exchange for money.

3.3 Contribution of the doctoral thesis

The main contribution of this doctoral thesis is the exploration of the two suggested options for connecting the Local Vertical Datums to the Global Vertical Reference Frame at the cm level precision.

Both presented strategies for connecting the LVDs to the GVRS are based on solving the geodetic boundary value problem. Hence, both methods can be applied on multiple disjointed LVDs and provide the connection corrections. The first proposed method is more suitable for inland countries, but it is very reliable when it comes to determination of the LVDs offsets. The second proposed method is a more general method because with the use of altimetry data it can be also used for island countries or it can be used offshore. Also, the combination of GGFM with the RTM technique can be used to thicken the data for remote areas or areas with some form of restricted accessibility.

3.4 PHYSGEO package

The PHYSGEO package is the software created and used for all the computation of this doctoral thesis. The whole package has more than 25 000 lines of code written in C++ and Python and it was given out free of charge under MIT licence. The package PHYSGEO is capable of computing

- the synthesis from GGFMs,
- the synthesis from GGFMs using the gradient approach (using the expansion of the functionals into Taylor's series),
- the gravity field modelling from DEMs (constant mass density or raster with mass density values),
- Residual Terrain Modelling,
- solving the Stokes' and Hotine's integrals in closed form or in the spectral form using the 'convolution' algorithm,
- creation of various plots of the results.

The code devoted to computing all previously mentioned tasks is written in C++ using the OpenMP project for multi-threading and parallel computations using the CPU. Most of the algorithms used are optimized for a good performance. For displaying the results, the Python code is available. Since all of the source codes are given away, anyone can modify them for their own need and use.

LITERATURA

- [1] BURŠA, M., RADĚJ, K., ŠÍMA, Z., TRUE, S. and VATRT, V. (1997). Tests for accuracy of recent geopotential models. *International Geoid Service Bulletin No*, **6**, 167–188.
- [2] BURŠA, M., GROTEN, E., KENYON, S., KOUBA, J., RADĚJ, K., VATRT, V. and VOJTÍŠKOVÁ, M. (2002). Earth's dimension specified by geoidal geopotential. *Studia Geophysica et Geodaetica*, **46**(1), 1–8. ISSN 1573-1626. doi: 10.1023/A:1020014930573. URL <https://doi.org/10.1023/A:1020014930573>.
- [3] BURŠA, M., KENYON, S., KOUBA, J., ŠÍMA, Z., VATRT, V. and VOJTÍŠKOVÁ, M. (2004). A Global Vertical Reference Frame Based on Four Regional Vertical Datums. *Studia Geophysica et Geodaetica*, **48**(3), 493–502. ISSN 1573-1626. doi: 10.1023/B:SGEG.0000037468.48585.e6. URL <https://doi.org/10.1023/B:SGEG.0000037468.48585.e6>.
- [4] SÁNCHEZ, L., ČUNDERLÍK, R., DAYOUB, N., MIKULA, K., MINARECHOVÁ, Z., ŠÍMA, Z., VATRT, V. and VOJTÍŠKOVÁ, M. (2016). A conventional value for the geoid reference potential W_0 . *Journal of Geodesy*, **90**(9), 815–835.
- [5] BALMINO, G., RUMMEL, R., VISSER, P. and WOODWORTH, P. (1999). Gravity field and steady-state ocean circulation mission. Technical report, Institut für Astronomische und Physikalische Geodäsie.
- [6] TAPLEY, B. D., BETTADPUR, S., WATKINS, M. and REIGBER, C. (2004). The gravity recovery and climate experiment: Mission overview and early results. *Geophysical research letters*, **31**(9).
- [7] REIGBER, C., LÜHR, H. and SCHWINTZER, P. (2002). CHAMP mission status. *Advances in Space Research*, **30**(2), 129–134.
- [8] MAYER-GÜRR, T., BEHZADPUR, S., ELLMER, M., KVAS, A., KLINGER, B., STRASSER, S. and ZEHENTNER, N. (2018). ITSG-Grace2018 - monthly, daily and static gravity field solutions from GRACE. *GFZ Data Services*. doi: 10.5880/ICGEM.2018.003. URL <http://doi.org/10.5880/ICGEM.2018.003>.
- [9] ZINGERLE, P., BROCKMANN, J. M., PAIL, R., GRUBER, T. and WILLBERG, M. (2019). The polar extended gravity field model TIM_R6e. *GFZ Data Services*. doi: 10.5880/ICGEM.2019.005.
- [10] FÖRSTE, C., BRUINSMAN, S., ABRIKOSOV, O., FLECHTNER, F., MARTY, J.-C., LEMOINE, J.-M., DAHLE, C., NEUMAYER, H., BARTHELMES, F., KÖNIG, R. ET AL. (2014). Eigen-6c4-the latest combined global gravity field model including goce data up to degree and order 1949 of gfz potsdam and grgs toulouse. In *EGU general assembly conference abstracts*, volume 16. GFZ Data Services. doi: 10.5880/icgem.2015.1.
- [11] GILARDONI, M., REGUZZONI, M. and SAMPIETRO, D. (2016). GECO: a global gravity model by locally combining GOCE data and EGM2008. *Studia Geophysica et Geodaetica*, **60**(2), 228–247. ISSN 1573-1626. doi: 10.1007/s11200-015-1114-4.
- [12] PAVLIS, N. K., HOLMES, S. A., KENYON, S. C. and FACTOR, J. K. (2008). An earth gravitational model to degree 2160: EGM2008. *EGU General Assembly*, **2008**(4), 4–2.
- [13] ZINGERLE, P., PAIL, R., GRUBER, T. and OIKONOMIDOU, X. (2019). The experimental gravity field model XGM2019e. *GFZ Data Services*. doi: 10.5880/ICGEM.2019.007. URL <http://dataservices.gfz-potsdam.de/icgem/showshort.php?id=escidoc:4529896>.
- [14] DANIELSON, J. J. and GESCH, D. B. (2010). Global Multi-resolution Terrain Elevation Data 2010 (GMTED2010). Technical report, U.S. Department of the Interior and U.S. Geological Survey. URL <https://pubs.usgs.gov/of/2011/1073/pdf/of2011-1073.pdf>.
- [15] BURŠA, M., KOUBA, J., MÜLLER, A., RADĚJ, K., TRUE, S. A., VATRT, V. and VOJTÍŠKOVÁ, M. (2001). Determination of Geopotential Differences between Local Vertical Datums and Realization of a World Height System. *Studia Geophysica et Geodaetica*, **45**(2), 127–132. ISSN 1573-1626. doi: 10.1023/A:1021860126850. URL <https://doi.org/10.1023/A:1021860126850>.
- [16] BURŠA, M., KENYON, S., KOUBA, J., ŠÍMA, Z., VATRT, V. and VOJTÍŠKOVÁ, M. (2004). A global vertical reference frame based on four regional vertical datums. *Studia geophysica et geodaetica*, **48**(3), 493–502.
- [17] SÁNCHEZ, L. (2009). Strategy to establish a global vertical reference system. In *Geodetic reference frames*, pages 273–278. Springer Berlin Heidelberg, Berlin, Heidelberg. ISBN 978-3-642-00860-3. doi: 10.1007/978-3-642-00860-3_42. URL https://doi.org/10.1007/978-3-642-00860-3_42.
- [18] SACHER, M., LIEBSCH, G., IHDE, J. and MÄKINEN, J. (2009). EVRF2007 as realization of the European Vertical Reference System. In *AGU Spring Meeting Abstracts*, pages 1–1.
- [19] FEATHERSTONE, W. (2000). Towards the unification of the Australian height datum between mainland and Tasmania using GPS and AUSGeoid98. *Geomatics Research Australasia*, **73**, 33–54.
- [20] TENZER, R., VATRT, V., GAN, L., ABDALLA, A. and DAYOUB, N. (2011). Combined approach for the unification of levelling networks in New Zealand. *Journal of Geodetic Science*, **1**(4), 324–332.
- [21] MERRY, C. L. (2007). An updated geoid model for Africa. In *Presented at Symposium G2, XXIV General Assembly of the IUGG*, volume 2.
- [22] DREWES, H., FORTES, L., HOYER, M. and BARRIGA, R. (1997). Status report on the sirgas project. *IGS 1996 Annual Report, 433-436, Pasadena*.
- [23] YOUNG, F. W. and MURAKAMI, J. (1989). The north american vertical datum of 1988 (navd '88) internal status report prepared for cism '88 winnipeg, manitoba may 24-27, 1988. *CISM Journal*, **43**(4), 387–393. doi: 10.1139/geomat-1989-0040.
- [24] RÜLKE, A., LIEBSCH, G., SACHER, M., SCHÄFER, U., SCHIRMER, U. and IHDE, J. (2012). Unification of European height system realizations. *Journal of Geodetic Science*, **2**(4), 343–354.
- [25] IHDE, J., BARZAGHI, R., MARTI, U., SÁNCHEZ, L., SIDERIS, M., DREWES, H., FÖRSTE, C., GRUBER, T., LIEBSCH, G. and PAIL, R. (2015). Report of the ad-hoc group on an international height reference system (ihrs). In: *Drewes H., Hornik H. (Eds.) Travaux de l'AIG 39, IAG Reports 2011-2015*.

- [26] SÁNCHEZ, L., DAYOUB, N., CUNDERLÍK, R., MINARECHOVÁ, Z., MIKULA, K., VATRT, V., VOJTÍŠKOVÁ, M. and SÍMA, Z. (2015). Report of joint working group 0.1. 1: vertical datum standardization (jwg 0.1. 1). In: *Drewes H., Hornik H.(Eds.) Travaux de l'AIG 39, IAG Reports 2011-2015*.
- [27] RUMMEL, R. (2000). Global integrated geodetic and geodynamic observing system (GIGGOS). In *Towards an integrated global geodetic observing system (IGGOS)*, pages 253–260. Springer Berlin Heidelberg, Berlin, Heidelberg. ISBN 978-3-642-59745-9.
- [28] GRUBER, T., GERLACH, C. and HAAGMANS, R. (2012). Intercontinental height datum connection with GOCE and GPS-levelling data. *Journal of Geodetic Science*, **2**(4), 270–280.
- [29] COLOMBO, O. L. (1980). A World Vertical Network. Technical report, OHIO STATE UNIV COLUMBUS DEPT OF GEODETIC SCIENCE.
- [30] GERLACH, C. and RUMMEL, R. (2013). Global height system unification with GOCE: a simulation study on the indirect bias term in the GBVP approach. *Journal of Geodesy*, pages 1–11. ISSN 1432-1394. doi: 10.1007/s00190-012-0579-y.
- [31] PEILIANG, X. and RUMMEL, R. (1991). Quality investigation of global vertical datum connection. *Publications on Geodesy*, **34**.
- [32] SANCHEZ, L. (2007). Definition and realisation of the SIRGAS vertical reference system within a globally unified height system. In *Dynamic planet*, pages 638–645. Springer.
- [33] ZHANG, L., LI, F., CHEN, W. and ZHANG, C. (2009). Height datum unification between Shenzhen and Hong Kong using the linearized fixed-gravimetric boundary value problem. *Journal of Geodesy*, **83**(5), 411–417.
- [34] BURŠA, M., KENYON, S., KOUBA, J., RADĚJ, K., VATRT, V., VOJTÍŠKOVÁ, M. and ŠIMEK, J. (2002). World height system specified by geopotential at tide gauge stations. In *Vertical Reference Systems*, pages 291–296. Springer Berlin Heidelberg, Berlin, Heidelberg. ISBN 978-3-662-04683-8.
- [35] BURŠA, M., ŠÍMA, Z., KENYON, S., KOUBA, J., VATRT, V. and VOJTÍŠKOVÁ, M. (2007). Twelve years of developments: Geoidal Geopotential W0 for the establishment of a World Height System—Present state and future. In *Proceedings of the 1st international symposium of the international gravity field service, Harita Genel Komutanligi, Istanbul*, pages 121–123.
- [36] JARVIS, A., REUTER, H. I., NELSON, A., GUEVARA, E. ET AL. (2008). Hole-filled SRTM for the globe Version 4. available from the CGIAR-CSI SRTM 90m Database (<http://srtm.csi.cgiar.org>).
- [37] STOKES, G. G. (1849). On the variation of gravity on the surface of the Earth. *Trans. Camb. Phil. Soc.*, **8**, 672–695.
- [38] HELMERT, F. R. (1884). *Die mathematischen und physikalischen theorieen der höheren geodäsie...*, volume 2. BG Teubner.
- [39] SOBOTÍKOVÁ, V. (2004). The finite element analysis of an elliptic problem with a nonlinear newton boundary condition. In Feistauer, M., Dolejší, V., Knobloch, P. and Najzar, K., editors, *Numerical Mathematics and Advanced Applications*, pages 766–774, Berlin, Heidelberg, 2004. Springer Berlin Heidelberg. ISBN 978-3-642-18775-9.
- [40] GREEN, G. (1854). An essay on the application of mathematical analysis to the theories of electricity and magnetism. *Journal für die reine und angewandte Mathematik*, **1854**(47), 161–221.
- [41] KELLOGG, O. D. (1953). *Foundations of potential theory*, volume 31. Courier Corporation.
- [42] DONNAY, J. D. (2011). *Spherical trigonometry*. Read Books Ltd.
- [43] LEBEDEV, N. N. (1965). *Special functions and their applications*. Prentice-Hall.
- [44] HUANG, J., SIDERIS, M. G., VANÍČEK, P. and TZIAVOS, I. N. (2003). Numerical investigation of downward continuation techniques for gravity anomalies. *Bollettino di geodesia e scienze affini*, **62**(1), 33–48. URL <http://www2.unb.ca/gge/Research/GRL/GeodesyGroup/Publications/documents/Numerical%20investigation%20of%20downward%20continuation.pdf>.
- [45] NOVÁK, P. and HECK, B. (2002). Downward continuation and geoid determination based on band-limited airborne gravity data. *Journal of Geodesy*, **76**(5), 269–278. ISSN 1432-1394. doi: 10.1007/s00190-002-0252-y.
- [46] SJÖBERG, L. E. (2003). A solution to the downward continuation effect on the geoid determined by Stokes’ formula. *Journal of Geodesy*, **77**(1-2), 94–100. ISSN 1432-1394. doi: 10.1007/s00190-002-0306-1.
- [47] HEISKANEN, W. A. and MORITZ, H. (1967). *Physical Geodesy*. W. H. Freeman and Company.
- [48] ZWILLINGER, D. (1997). Clairaut’s equation. *Handbook of Differential Equations, 3rd ed. Academic Press, Boston, MA*, **120**, 158–160.
- [49] NÁDENÍK, Z. (2000). *Kulové funkce pro geodézií: Matematická příprava ke studiu knihy W. A. Heiskanen - H. Moriz: Physical Geodesy, 1967 [in Czech Language]*. Výzkumný ústav geodetický, topografický a kartografický. ISBN 80-85881-15-2.
- [50] STRANG VAN HEES, G. (1992). Practical formulas for the computation of the orthometric and dynamic correction. *Zeitschrift für Vermessungswesen*, **117**.
- [51] HELMERT, F. R. (1890). Die schwerkraft im hochgebirge insbesondere in den tyroler alphen in geodatischer und geologischer beziehung. *shii*.
- [52] NIETHAMMER, T. (1932). *Nivellement und Schwere als Mittel zur Berechnung wahrer Meereshöhen; mit 25 Taf. Kartenverl. d. schweiz. Landestopographie in Komm.*
- [53] MADER, K. (1954). Die orthometrische schwerekorrektion des präzisions-nivellements in den hohen tuaern. *ospn*.
- [54] VANÍČEK, P., KLEUSBERG, A., MARTINEC, Z., SUN, W., ONG, P., NAJAFI, M., VAJDA, P., HARRIE, L., TOMÁŠEK, P. and HORST, B. (1995). Compilation of a precise regional geoid. *Final report on research done for the Geodetic Survey Division, Fredericton*.

- [55] FEATHERSTONE, W. and ALLISTER, N. (2001). Estimation of helmert orthometric heights using digital barcode levelling, observed gravity and topographic mass-density data over part of the darling scarp, western australia. *Geomatics Research Australasia*, **75**, 25–52.
- [56] HWANG, C.-W. and HSIAO, Y.-S. (2003). Orthometric corrections from leveling, gravity, density and elevation data: a case study in taiwan. *Journal of Geodesy*, **77**(5-6), 279–291.
- [57] KRARUP, T. (1969). A contribution to the mathematical foundation of physical geodesy. *MeGIC*, **44**.
- [58] MORITZ, H. (1977). Recent developments in the geodetic boundary value problem. Technical report, OHIO STATE UNIV COLUMBUS DEPT OF GEODETIC SCIENCE.
- [59] SANZO, F. (1978). Molodensky's problem in gravity space: a review of the first results. *Bulletin Géodésique*, **52**(1), 59–70.
- [60] MACÁK, M., MINARECHOVÁ, Z. and MIKULA, K. (2014). A novel scheme for solving the oblique derivative boundary-value problem. *Studia Geophysica et Geodaetica*, **58**(4), 556–570.
- [61] ČUNDERLÍK, R., MACÁK, M., MEDL'A, M., MIKULA, K. and MINARECHOVÁ, Z. (2019). *Numerical Methods for Solving the Oblique Derivative Boundary Value Problems in Geodesy*, pages 1–48. Springer Berlin Heidelberg, Berlin, Heidelberg. ISBN 978-3-662-46900-2. doi: 10.1007/978-3-662-46900-2_105-1. URL https://doi.org/10.1007/978-3-662-46900-2_105-1.
- [62] SCHWARZ, K. P., SIDERIS, M. G. and FORSBERG, R. (1990). The use of FFT techniques in physical geodesy. *Geophysical Journal International*, **100**(3), 485–514. ISSN 0956-540X. doi: 10.1111/j.1365-246X.1990.tb00701.x. URL <https://doi.org/10.1111/j.1365-246X.1990.tb00701.x>.
- [63] MORITZ, H. (1980). Advanced physical geodesy. *Advances in Planetary Geology*.
- [64] DENKER, H. and TZIAVOS, I. (1999). Investigation of the molodensky series terms for terrain reduced gravity field data. *Bollettino di Geofisica Teorica ed Applicata*, **40**(3-4), 195–203.
- [65] LI, Y. C., SIDERIS, M. G. and SCHWARZ, K.-P. (1995). A numerical investigation on height anomaly prediction in mountainous areas. *Bulletin géodésique*, **69**(3), 143–156.
- [66] FORSBERG, R. and TSCHERNING, C. C. (1981). The use of height data in gravity field approximation by collocation. *Journal of Geophysical Research: Solid Earth*, **86**(B9), 7843–7854. doi: 10.1029/JB086iB09p07843. URL <https://agupubs.onlinelibrary.wiley.com/doi/abs/10.1029/JB086iB09p07843>.
- [67] BACKUS, G. E. (1968). Application of a non-linear boundary-value problem for Laplace's equation to gravity and geomagnetic intensity surveys. *The Quarterly Journal of Mechanics and Applied Mathematics*, **21**(2), 195–221.
- [68] BJERHAMMAR, A. and SVENSSON, L. (1983). On the geodetic boundary value problem for a fixed boundary surface—a satellite approach. *Bulletin géodésique*, **57**(1-4), 382–393.
- [69] HECK, B. (1989). On the non-linear geodetic boundary value problem for a fixed boundary surface. *Bulletin géodésique*, **63**(1), 57–67.
- [70] HOTINE, M. (1969). Mathematical geodesy. *Washington, US Environmental Science Services Administration; [for sale by the Supt. of Docs., US Govt. Print. Off.] 1969*.
- [71] LI, F., CHEN, W. and YUE, J. (2003). On solution and application of GPS/gravity boundary value problem. *Chinese Journal of Geophysics*, **46**(5), 851–858. doi: 10.1002/cjg2.405. URL <https://agupubs.onlinelibrary.wiley.com/doi/abs/10.1002/cjg2.405>.
- [72] HECK, B. (1990). An evaluation of some systematic error sources affecting terrestrial gravity anomalies. *Bulletin Géodésique*, **64**(1), 88–108.
- [73] HOFMANN-WELLENHOF, B. and MORITZ, H. (2005). *Physical geodesy*. Springer. ISBN 3211235841. doi: 10.1007/b139113.
- [74] BURŠA, M., KOUBA, J., KUMAR, M., MÜLLER, A., RADĚJ, K., TRUE, S. A., VATRT, V. and VOJTÍŠKOVÁ, M. (1999). Geoidal Geopotential and World Height System. *Studia Geophysica et Geodaetica*, **43**(4), 327–337. ISSN 1573-1626. doi: 10.1023/A:1023273416512. URL <https://doi.org/10.1023/A:1023273416512>.
- [75] PIZZETTI, P. (1894). *Sulla espressione della gravità alla superficie del geoide supposto ellissoidico*. Tip. della R. Accademia dei Lincei.
- [76] SOMIGLIANA, C. (1930). *Sul campo gravitazionale esterno del geoide ellissoidico*.
- [77] JEREMEJEV, V. F. and JURKINA, M. I. (1974). *Teorija vysot v gravitacionnom poli Zemli [in Russian language]*. Nėdra Moskva.
- [78] IHDE, J., AUGATH, W. and SACHER, M. (2002). The Vertical Reference System for Europe. In Drewes, H., Dodson, A. H., Fortes, L. P. S., Sánchez, L. and Sandoval, P., editors, *Vertical Reference Systems*, pages 345–350, Berlin, Heidelberg, 2002. Springer Berlin Heidelberg. ISBN 978-3-662-04683-8.
- [79] PETIT, G. and LUZUM, B. (2010). IERS Conventions (2010). Technical report, BUREAU INTERNATIONAL DES POIDS ET MESURES SEVRES (FRANCE).
- [80] POUTANEN, M., VERMEER, M. and MÄKINEN, J. (1996). The permanent tide in GPS positioning. *Journal of Geodesy*, **70**(8), 499–504.
- [81] MÄKINEN, J. and IHDE, J. (2009). The Permanent Tide in Height Systems. In Sideris, M. G., editor, *Observing our Changing Earth*, pages 81–87, Berlin, Heidelberg, 2009. Springer Berlin Heidelberg. ISBN 978-3-540-85426-5.
- [82] EKMAN, M. (1989). Impacts of geodynamic phenomena on systems for height and gravity. *Bulletin Géodésique*, **63**(3), 281–296. ISSN 1432-1394. doi: 10.1007/BF02520477. URL <https://doi.org/10.1007/BF02520477>.
- [83] EINSTEIN, A. (1911). On the Influence of Gravitation on the Propagation of Light. *Ann. Phys.*, **35**, 898–908.

- [84] TSCHERNING, C. (1984). The geodesist's handbook 1984. *Bulletin géodésique*, **58**(3), 219–463.
- [85] HEIKKINEN, M. (1978). On the tide-generating forces, publ. *Finnish Geodetic Inst*, **85**, 1–150.
- [86] KADLEC, M. (2012). *Modely tíhového pole země s vysokým rozlišením a terénní efekty*. PhD thesis, Západočeská univerzita v Plzni.
- [87] GROMBEIN, T., SEITZ, K. and HECK, B. (2013). Optimized formulas for the gravitational field of a tesseroid. *Journal of Geodesy*, **87**(7), 645–660. ISSN 1432-1394. doi: 10.1007/s00190-013-0636-1. URL <https://doi.org/10.1007/s00190-013-0636-1>.
- [88] HECK, B. and SEITZ, K. (2007). A comparison of the tesseroid, prism and point-mass approaches for mass reductions in gravity field modelling. *Journal of Geodesy*, **81**(2), 121–136. ISSN 1432-1394. doi: 10.1007/s00190-006-0094-0. URL <https://doi.org/10.1007/s00190-006-0094-0>.
- [89] DENKER, H. (2013). Regional gravity field modeling: theory and practical results. In *Sciences of Geodesy - II: Innovations and Future Developments*, pages 185–291. Springer Berlin Heidelberg, Berlin, Heidelberg. ISBN 978-3-642-28000-9. doi: 10.1007/978-3-642-28000-9_5. URL https://doi.org/10.1007/978-3-642-28000-9_5.
- [90] MÄRDLA, S., ÅGREN, J., STRYKOWSKI, G., OJA, T., ELLMANN, A., FORSBERG, R., BILKER-KOIVULA, M., OMANG, O., PARŠELIŪNAS, E., LIEPINS, I. and KAMINSKIS, J. (2017). From discrete gravity survey data to a High-resolution Gravity Field Representation in the Nordic-Baltic region. *Marine Geodesy*, **40**(6), 416–453. doi: 10.1080/01490419.2017.1326428. URL <https://doi.org/10.1080/01490419.2017.1326428>.
- [91] HIRT, C. (2010). Prediction of vertical deflections from high-degree spherical harmonic synthesis and residual terrain model data. *Journal of Geodesy*, **84**(3), 179–190. ISSN 1432-1394. doi: 10.1007/s00190-009-0354-x. URL <https://doi.org/10.1007/s00190-009-0354-x>.
- [92] HIRT, C. and KUHN, M. (2014). Band-limited topographic mass distribution generates full-spectrum gravity field: Gravity forward modeling in the spectral and spatial domains revisited. *Journal of Geophysical Research: Solid Earth*, **119**(4), 3646–3661. doi: 10.1002/2013JB010900. URL <https://agupubs.onlinelibrary.wiley.com/doi/abs/10.1002/2013JB010900>.
- [93] HIRT, C., GRUBER, T. and FEATHERSTONE, W. (2011). Evaluation of the first GOCE static gravity field models using terrestrial gravity, vertical deflections and EGM2008 quasigeoid heights. *Journal of geodesy*, **85**(10), 723–740.
- [94] HIRT, C., CLAESSENS, S., FECHER, T., KUHN, M., PAIL, R. and REXER, M. (2013). New ultrahigh-resolution picture of Earth's gravity field. *Geophysical Research Letters*, **40**(16), 4279–4283. doi: 10.1002/grl.50838. URL <https://agupubs.onlinelibrary.wiley.com/doi/abs/10.1002/grl.50838>.
- [95] VERGOS, G. S., EROL, B., NATSIPOULOS, D. A., GRIGORIADIS, V. N., IŞIK, M. S. and TZIAVOS, I. N. (2018). Preliminary results of GOCE-based height system unification between Greece and Turkey over marine and land areas. *Acta Geodaetica et Geophysica*, **53**(1), 61–79.
- [96] HIRT, C., KUHN, M., CLAESSENS, S., PAIL, R., SEITZ, K. and GRUBER, T. (2014). Study of the Earth's short-scale gravity field using the ERTM2160 gravity model. *Computers & geosciences*, **73**, 71–80. ISSN 00983004. doi: 10.1016/j.cageo.2014.09.00.
- [97] FORSBERG, R. (1984). A study of terrain reductions, density anomalies and geophysical inversion methods in gravity field modelling. Technical report, Ohio State Univ Columbus Dept Of Geodetic Science and Surveying.
- [98] FORSBERG, R. (2009). Terrain modelling with ultra-high resolution spherical harmonic geopotential models. In *Presented at Geodesy for planet Earth, IAG, Buenos Aires*, pages 1–10.
- [99] OMANG, O. C., TSCHERNING, C. C. and FORSBERG, R. (2012). Generalizing the harmonic reduction procedure in residual topographic modeling. In *VII Hotine-Marussi Symposium on Mathematical Geodesy*, pages 233–238. Springer.
- [100] PAVLIS, N. (2008). EGM2008 - WGS 84 Version. URL https://earth-info.nga.mil/GandG//wgs84/gravitymod/egm2008/egm08_wgs84.html.
- [101] ČESKÝ ÚŘAD ZEMĚMĚŘICÍ A KATASTRÁLNÍ (2013). Podrobný kvazigeoid QGZÚ 2013. URL [https://geoportal.cuzk.cz/\(S\(0ob0jpyif3oluacmrno40xd1\)\)/Default.aspx?mode=TextMeta&side=bodpole&metadataID=CZ-CUZK-QGZU&menu=275](https://geoportal.cuzk.cz/(S(0ob0jpyif3oluacmrno40xd1))/Default.aspx?mode=TextMeta&side=bodpole&metadataID=CZ-CUZK-QGZU&menu=275).
- [102] KLOBUŠIAK, M., LEITMANNOVÁ, K. and FERIANC, D. (2005). Realizácia záväzných transformácií národných referenčných súradnicových a výškového systému do Európskeho Terestrického referenčného Systému 1989 [in slovak language]. In *Geodetické siete a priestorové informácie, SSGK*, pages 1–1. GKÚ a TOPU Banská Bystrica.
- [103] ŠAMAJOVÁ, L. and JOZEK, H. (2018). Hustota horninových komplexov Západných Karpát na území Slovenska [in slovak language]. Technical report, Comenius University in Bratislava. URL https://www.geology.sk/wp-content/uploads/2019/03/02_GPS-132-Samajova-Hok.pdf.

PUBLICATIONS OF THE AUTHOR

JOURNAL ARTICLES (REFEREED)

- Štěpánek, P.; Hugentobler, U.; **Buday, M.**; Filler, V.: Estimation of the Length of Day (LOD) from DORIS observations. *Advances in Space Research*, year 62, num. 2, 2018: p. 370–382, doi:<https://doi.org/10.1016/j.asr.2018.04.038>. URL <http://www.sciencedirect.com/science/article/pii/S0273117718303703>
- Bartonek, D.; **Buday, M.**: Problems of Creation and Usage of 3D Model of Structures and Theirs Possible Solution. *Symmetry*, year 12, num. 1, 2020: pages. 181, doi: 10.3390/sym12010181. URL <https://www.mdpi.com/2073-8994/12/1/181>
- **Buday, M.**: Transformácia lokálneho výškového systému (Baltský po vyrovnaní) do jednotného celosvetového výškového systému. *Geodetický a kartografický obzor* [in Slovak language], year 10, 2017, ISSN 0016-7096.
- **Buday, M.**; Štěpánek, P.; Filler, V.; et.al.: Určovanie parametra skutočnej dĺžky dňa LOD z meraní DORIS a analýza jeho časových radov [in Slovak Language]. *Geodetický a kartografický obzor*, year 8, 2017, ISSN 0016-7096.
- Vatr, V.; Machotka, R.; **Buday, M.**: Kronstadt Height Datum on the Territories of the Czech and Slovak Republics and its Connection to a Global Vertical Reference Frame. *In Advances and Trends in Geodesy, Cartography and Geoinformatics: Proceedings of the 10th International Scientific and Professional Conference on Geodesy, Cartography and Geoinformatics (GCG 2017)*, Taylor & Francis group: Taylor & Francis group, april 2018, ISBN 978-1-138-58489-1, p. 139–147.
- Kratochvíl, R.; Machotka, R.; **Buday, M.**: Use of the topographic deflections of the vertical for computation of the quasigeoid. *In Advances and Trends in Geodesy, Cartography and Geoinformatics II: Proceedings of the 11th International Scientific and Professional Conference on Geodesy, Cartography and Geoinformatics (GCG 2019)*, September 10-13, 2019, Demänovská Dolina, Low Tatras, Slovakia, editation S. Molčíková; V. Hurčíková; P. Blištan, 2020, ISBN 978-0-429-32702-5, doi: 10.1201/9780429327025.

CONFERENCE ARTICLES (REFEREED)

- **Buday, M.**: Transformation of the local height system (Baltic vertical Datum) into unified World Height System. *In conference proceedings Juniorstav 2017*, 2017, ISBN 978-80-214-5462-0.
- **Buday, M.**: The quasigeoid rectification in Central Bohemia. *In SKN Sejmik meeting - Wroclaw*, 2017, ISBN 978-83-7717-259-9.
- Kratochvíl, R.; Volařík, T.; **Buday, M.**: Interpolace Astrogeodetických Tížnicových Odchylek Pomocí Topografických Tížnicových Odchylek [in Czech language]. *In conference proceedings Juniorstav 2017*, 2017, ISBN 978-80-214-5462-0.
- **Buday, M.**: Posudenie využitia presneho merania času pri zjednocovaní výškových systemov [in Slovak Language]. *In conference proceedings Juniorstav 2017*, 2017, ISBN 978-80-214-5311-1, ISSN 1190-1535.
- **Buday, M.**; Vatr, V.; Machotka, R.: The numerical evaluation of geoid-quasigeoid separation for the Czech Republic and the Slovak Republic. *In Družicové metody v geodezii a katastru*, ECON Publishing s.r.o.: ECON Publishing s.r.o., january 2019, ISBN 978-80-86433-72-1, p. 68–72.
- **Buday, M.**: Transformation of the local height system (Baltic vertical Datum) into unified World Height System. *In conference proceedings Juniorstav 2017*, Brno University of Technology, january 2017, ISBN 978-80-2145473-6
- Vatr, V.; Machotka, R.; **Buday, M.**: Kronstadt Height Datum connection to Global Vertical System - territories of the Czech and Slovak Republics example. *In 5th Czech-Polish symposium ACTUAL PROBLEMS OF GEODESY, CARTOGRAPHY AND PHOTOGRAMMETRY*, june 2017, ISBN 978-80-86433-66-0
- Kratochvíl, R.; Machotka, R.; **Buday, M.**: Use of the topographic deflections of the vertical for computation of the quasigeoid. *In Advances and Trends in Geodesy, Cartography and Geoinformatics II: Proceedings of the 11th International Scientific and Professional Conference on Geodesy, Cartography and Geoinformatics (GCG 2019)*, September 10-13, 2019, Demänovská Dolina, Low Tatras, Slovakia, editation S. Molčíková; V. Hurčíková; P. Blištan, 2020, ISBN 978-0-429-32702-5, doi: 10.1201/9780429327025.

ABSTRACTS

- **Buday, M.**; Štěpánek, P.; Filler, V.: DORIS research activities at Geodetic Observatory Pecny.

- In EGU General Assembly Conference Abstracts, year 19, 2017,*
- Štěpánek, P.; Filler, V.; **Buday, M.**; Hugentobler, U.: LOD estimation from DORIS observations. *In EGU General Assembly Conference Abstracts, year 18, 2016*
 - Štěpánek, P.; Filler, V.; **Buday, M.**: Recent DORIS analysis at Geodetic Observatory Pecny. *In IDS Workshop, La Rochelle France, 2016.*
 - Štěpánek, P.; **Buday, M.**; Filler, V.: DORIS research activities at Geodetic Observatory. *In IAG-IASPEI Joint scientific Assembly of the International Association of Geodesy and the International Association of Seismology and Physics of the Earth's Interior, 2017*
 - Štěpánek, P.; **Buday, M.**; V., F.: Length of the Day estimated from DORIS observations. *In IAG-IASPEI Joint scientific Assembly of the International Association of Geodesy and the International Association of Seismology and Physics of the Earth's Interior, 2017*
 - Vátrt, V.; Machotka, R.; Jurčík, J.; **Buday, M.**: Praktické aplikace aktuální hodnoty potenciálu na geoidu po jejím projednání na 26. valném zasedání IUGG. october 2015.
 - **Buday, M.**; Vátrt, V.; Pospíšil, L.: Computation of the quasigeoid-geoid separation for the territories of the Czech Republic and the Slovak Republic. *In GRAVITY, GEOID and HEIGHT SYSTEMS 2, Denmark DTU Space, september 2018*

CURRICULUM VITAE

PERSONAL INFORMATION

Name Michal
Surname Buday
Email buday.m@fce.vutbr.cz
buday2@gmail.com

WORK EXPERIENCE

Jan. 2018 – Sep. 2020 Faculty of Civil Engineering, Brno University of Technology,
Czech Republic

Work position Assistant lecturer
*An employee of the Faculty of Civil Engineering with focus on research of the Earth's gravity field.
Creating software in C++.*

Jan. 2016 - Dec. 2017 Research Institute of Geodesy, Topography and Cartography,
Prague, Czech Republic

Work position A research worker in the field of geodynamics and geodesy
*Part-time job (0,5) on project MSMT (LG15018) – Optimization of models applied in determination of
physical and geodetic parameters from DORIS measurements - time series analysis. Creating software
in C++.*

EDUCATION

June 2015 - Present Faculty of Civil Engineering, Brno University of Technology
Doctoral programme: Geodesy and Cartography

July 2013 - June 2015 Faculty of Civil Engineering, Brno University of Technology
*Master's programme: Geodesy and Cartography
Attained medal SIGNUM PROSPERITATIS for excellent
study results*

Sep. 2010 - June 2013 Faculty of Civil Engineering, Brno University of Technology
Bachelor's programme: Geodesy and Cartography

Sep. 2002 - May 2010 Grammar school of Jozef Branecký, Trenčín, Slovakia
Graduation/secondary school-leaving exam.

PC SKILLS

Basic knowledge:

- MATLAB, SCILAB
- QGIS
- Microstation, AutoCAD
- L^AT_EX
- MS Office, Libre Office
- programming languages: BASH

Intermediate knowledge:

- Linux OS (FEDORA, UBUNTU)
- programming languages: C++, Python

LANGUAGE SKILLS

- English language - upper intermediate (written and spoken), B2 (Common European Framework of Reference for Languages)
- Italian language - beginner (written and spoken)
- Slovak language - mother tongue

OTHER SKILLS

- Driving license category: AM, B

ABSTRACT

One of the main problems of current physical geodesy is the unification of local height systems and the creation of the unified global vertical reference frame, whose primary definition constant will be the geopotential value of W_0 on the level surface, such as geoid. This problem encounters several pitfalls, such as different types of physical heights used in the world, ways of eliminating the effects of tides on the shape of the Earth's body, or the ability to agree internationally on a reference value of W_0 .

This thesis is divided into two main parts. The first part is a description of the theoretical foundations concerning the description of the Earth's gravitational field, the basics of height theory and the description of the Newton's boundary value problem and Neumann boundary value problem, together with the solution of the Hotine's and Stokes' integral. Due to the fact that the data of directly measured gravity acceleration for the territory of the Czechia and the Slovakia are not freely available with sufficient coverage, these data were replaced by gravity disturbances calculated from the Global Gravity Model of the Earth. To improve the data obtained from geopotential models, so-called residual terrain modelling was used. It is a spectral combination of gravity field models with relevant Earth's gravitational field quantities, which are obtained by modelling from a digital terrain model and a height model that represents the mean value of topography. The combination of these data consists of calculating those frequencies of the gravitational signal from the digital terrain model that are not a part of the signal obtained from geopotential models that in general have a lower spatial resolution.

Two methods were used to connect the local height systems of the Czech Republic and the Slovak Republic. The first method was to use the solution of Molodensky's problem. Input data were gravity disturbances that were calculated from various global geopotential models. Subsequently, the solution using the combination of data mentioned in the previous paragraph was also calculated. The second method used is originally a method developed to test geopotential models. The disadvantage of this method is that it relies only on GNSS/levelling points. Both methods were tested on a set of measuring points (GNSS/levelling points) and their results are tabled in the second part of the thesis which is focused on the summary of the results. Practical calculations have shown that the offset of the height systems for both republics is almost identical, with a maximum difference of 3 cm, using the same input data. However, the plane approximation shows that the tilt value differs for different height systems. At the same time, the results combining the global gravity field model with the residual terrain modelling technique provide improved behaviour in mountainous areas.

The results of the doctoral thesis are accompanied by a programmed package of functions written in the C++. This package can compute the synthesis of gravity parameters from global gravity models, model the Earth's gravitational field from a digital terrain model, solve the Stokes integral and many others. All source codes can be found on the enclosed DVD as an attachment to this thesis. All the source codes are also available free of charge under MIT licence on: <https://gitlab.com/buday2/physgeo..>

KEYWORDS

physical geodesy, physical heights, geodetic boundary value problem, residual terrain modelling, height system unification

BUDAY, Michal. *Geophysical methods of integration of the local vertical datums into World Height System*. Brno, 2020, 44 p. Treatise on doctoral thesis. Brno University of Technology, Faculty of Civil Engineering, Department of Geodesy. Supervised by prof. Ing. Viliam Vatrť, DrSC.